Pteryxin suppresses hepatocellular carcinoma by targeting HIF-1α and glucose metabolism

Author

Yueyang Wang

School

International Department,
The Affiliated High School of South China Normal University

Supervisor

Linchong Sun, Ph. D
（South China University of Technology, Associate Professor）

Location

Guangzhou

Table of Contents

Pteryxin suppresses hepatocellular carcinoma by targeting HIF-1α and glucose metabolism

Yueyang Wang, International Department of the Affiliated High School of South China Normal University

Abstract

The development of new anti-cancer drugs from Chinese herbal compounds is drawing much attention in the field of cancer therapy. In this study, we performed a small scale drug screening to identify potential anti-cancer herbal compounds. As a result, we found that Pteryxin, extracted from the plant *Peucedanum praeruptorum Dunn*, exhibited strong anti-tumor effects. Pteryxin inhibits cell proliferation in multiple hepatocellular carcinoma cell lines, including Hep3B, HepG2 and PLC. More interestingly, this inhibitory effect is much more potent under hypoxic conditions. Mechanistic analysis revealed that Pteryxin suppresses the expression of HIF-1α (hypoxia-inducible factor 1α) at protein level as well as the expression of glucose metabolic enzymes at both mRNA and protein levels, suggesting that Pteryxin suppresses HIF-1α-mediated glucose metabolism. Moreover, mice xenograft experiments showed that Pteryxin efficiently prevented tumor initiation and inhibited tumor progression *in vivo*. Importantly, Pteryxin markedly inhibited the proliferation of clinical human liver cancer patient-derived organoids by targeting glucose metabolism, with marginal effect on the normal liver-derived organoids, indicating its specific toxic effect on tumor tissues and high anti-cancer implication potentials.

Collectively, Pteryxin efficiently suppresses liver cancer progression by inhibiting HIF-1α and hypoxia-activated glucose metabolism both *in vitro* and *in vivo*, presenting a new potential herbal compound for tumor prevention and anti-cancer therapy. Thus, the potential for the clinical application of our Chinese herbal compound, Pteryxin, warrants further study.

Key Words: Chinese herbal medicines, Pteryxin, hepatocellular carcinoma, hypoxia, glucose metabolism

Statement of Originality

I, Yueyang Wang, declare that this research is conducted under the guidance of the supervisor/instructor and that our original work, conducted especially for the purpose and objectives of this study, has not been previously submitted or published elsewhere.

Signature: Yueyang Wang

Date：09/12/2019

1. Introduction (Research background and objectives)

Cancer is one of the most common diseases that threaten our life and accounts for 1/4 of all the deaths. Due to the severe toxicity and limited therapeutic effects of many anti-cancer drugs, scientists and clinicians are looking for alternative therapies. In this regard, Chinese herbal medicine has drawn much attention over the recent years. Pteryxin is an effective herbal extract and it is mainly extracted from umbelliferae plants *Peucedanum praeruptorum Dunn* and *Seseli mairei* grown in Sichuan, Guizhou, and Guangxi in south-west China [1-2]. Early study discovered that Pteryxin inhibited NO production in lipopolysaccharide (LPS)-induced mouse peritoneal derived macrophages to exhibit anti-inflammatory effect [3]. Nugara *et al.* found that Pteryxin enhanced the genes of *de novo* fatty acid synthesis and inhibited the genes of fatty acid oxidation to inhibit obesity, and Pteryxin is thus regarded as a potential diet drug [4]. In mouse models, pharmacokinetics study of Pteryxin indicated that Pteryxin circulated into plasma, intestines, stomach, spleen, kidney, liver, heart and brain through oral administration. Due to the low polarity, Pteryxin could pass the blood-brain barrier easily [5]. Furthermore, Pteryxin can enhance the resistance of rice to rice blast and cold [6]. Interestingly, while Pteryxin has been known for multiple functions, its effect on cancer progression has never been documented.

During the proliferation of solid tumors, the interior of tumor cells is often surrounded by a low oxygen microenvironment, the so-called hypoxic microenvironment. Under hypoxia, cancer cells induce the expression of an important transcription factor HIF-1α that regulates cell proliferation, apoptosis, metabolism, migration, and autophagy of cells to help cancer cells adapt the tumor hypoxic microenvironment [7-8]. On the other hand, metabolic disorder is one of the important characteristics in cancers. The most classical metabolic change is Warburg Effect, leading tumor cells to use glycolysis by converting glucose to pyruvate and lactate to generate ATP. During glucose metabolism, most glycolytic enzymes are up-regulated by HIF-1α and are highly activated in cancers [9-10]. However, little is known about whether Pteryxin affects cancer progression through metabolic reprogramming under hypoxic conditions

In this study, we performed a small scale drug screening to identify potential anti-cancer herbal compounds. As a result, we found that Pteryxin, extracted from the plant *Peucedanum praeruptorum Dunn*, exhibited strong anti-tumor effects. Pteryxin significantly inhibited the proliferation of multiple hepatocellular carcinoma cells, and the inhibitory effect became more potent under hypoxic conditions. Mechanistic study revealed that Pteryxin decreased the protein expression of HIF-1α and HIF-1α-regulated glucose metabolic enzymes. Furthermore, in mouse xenograft experiments, Pteryxin suppressed the initiation and progression of hepatocellular carcinoma by inhibiting HIF-1α and glucose metabolic enzymes. More importantly, by using organiod models, we found that Pteryxin inhibited the growth of clinical human liver cancer patient-derived tumor organiods, with very mild toxic effects on the normal liver-derived organiods. These results indicate that Pteryxin can inhibit hepatocellular carcinoma progression both *in vitro* and *in vivo*, suggesting that Pteryxin is a potential herbal compound to target tumor growth. Thus, this study provides important evidence for the anti-cancer effect of the herbal compound, Pteryxin.

2. Materials and Experimental Methods

2.1 Cell culture and Reagents

Human hepatocellular carcinoma cell lines Hep3B, PLC and HepG2 (purchased from ATCC) were cultured in DMEM supplemented with 10% fetal bovine serum and 1% penicillin-streptomycin in 37℃, 5% CO_2 incubator. For Pteryxin or hypoxia treatment, cells were cultured with Pteryxin or under hypoxic work station (1% O_2, 5% CO_2, 94% N_2, Don Whitley Scientific) for the indicated time.

For Western blot assay, HIF-1α, LDHA, PKM2, GLUT1 and Actin antibodies were all purchased from Proteintech Group, Wuhan. For drug treatment assay, DMOG, DFX, $CoCl_2$ and MG-132 were purchased from Targetmol, Shanghai.

2.2 Herbal compound library and Drug screening

Herbal compound library including 29 herbal compounds was purchased from

Targetmol, Shanghai. These compounds are mainly extracted from Chinese herbs such as *Scutellaria baicalensis* (黄芩), *Astragalus membranaceus* (黄芪), *Slvia miltiorrhiza Bunge* (丹参), *Peucedanum decursivum Maxim.* (紫花前胡), and *Cistanche deserticola* (肉苁蓉) that are very common throughout China and very accessible to ordinary people. Each compound was dissolved with DMSO and prepared into a stock solution. In each of the 24-well plates, 2 x 10^4 Hep3B cells were pre-seeded, and natural compounds with a working concentration of 100 uM were added to each of the wells after the cells were attached to the wall, and DMSO with equal dilution ratio was added as control. After 96 hours of treatment, the cells in each well are stained by crystal violet.

2.3 Crystal violet staining

After cell culture or drug treatment, the culture medium was discarded and carefully washed with PBS for 1-2 times to remove the residual culture medium; The cells were fixed with methanol for 20min, stained with 0.1 % crystal violet for 15-20 min, and washed off with PBS. After natural drying or drying at 37℃, the crystal violet stained cell culture plates were scanned by the scanner. The plates can be kept at room temperature for a long time. The positive staining represents remaining live cells, thus, less staining indicates more killing ability of the compounds. Note: crystal violet is prepared into 0.5% stock solution (0.5 g crystal violet was dissolved into 100 ml PBS), and diluted with PBS when used.

2.4 IC-50 measurement by MTT assay

2.4.1 Seed cells in 96-well plates

Blank: DMEM

Control group: cells＋DMEM

Treated group: cells＋DMEM＋Pteryxin

Suspend cells with DMEM that contains 10 % FBS and seed cells at 6000 per well with 100 ul of DMEM.

2.4.2 After 24 hours of incubation at 37℃ and 5 % CO_2, cells were treated with different doses of Pteryxin ranging from 400 uM to 3.125 uM by the double dilution method. 6

parallel wells were set up for each concentration and incubated at 37℃ and 5% CO_2 for another 48 hours treatment.

2.4.3 After 48 hours of treatment, 10 ul of MTT (5mg/ml) was added to each well of Blank, Control group and Treated groups, followed by incubation for 4 hours at 37℃ until the purple precipitate is visible, then 100 ul of triplex solution was added to each well to resolve the precipitate sufficiently.

2.4.4 The absorbance at 570 nm (OD570) of each well was measured by a micro-plate reader and the relative cell viability was calculated according to the following formula: [OD570 (Treated group) - OD570 (Blank)] / [OD570 (Control) - OD570 (Blank)]×100%. Then, IC50 was calculated by Graphpad Prism 7.0 using nonlinear regression according to the relative cell viability and corresponding doses.

2.5 Total RNA extraction and qRT-PCR

2.5.1 Extract total RNA using trizol

1) Wash cells with PBS in 6cm dish

2) Add 1 ml of trizol to lyse the cells and collect samples to EP tube

3) Add 200 ul of chloroform, mix well by inverting the tube 5~6 times. Sit on the bench for 2~3 min until separating into two layers

4) Centrifuge 8000 rpm for 15 min at 4°C

5) Add 500 ul of isopropanol in a new EP tube

6) Transfer the supernatant to the new EP tube with isopropanol, mix well by inverting the tube 5~6 times to precipitate the RNA

7) Centrifuge 10K rpm for 15 min at 4°C

8) Discard the supernatant and add 750 ul of 70 % ethanol to wash the RNA pellet

9) Spin down 10K rpm for 15 min at 4°C

10) Air dry for several minutes, add 40~100 ul of 0.1 % DEPC H_2O to dissolve the RNA and detect RNA concentration by using NanoDrop

2.5.2 cDNA synthesis using iScript™ cDNA synthesis kit

1) Set up reaction as bellow in 200 ul PCR tube:

Components	Volume per Reaction
5x iScript reaction mix	4 µl
iScript reverse transcriptase	1 µl
Nuclease-free water	(15-x) µl
RNA (1 µg total RNA)	x µl
Total volume	20 µl

2) PCR program:

5 minutes at 25°C

30 minutes at 42°C

5 minutes at 85°C

Hold at 4°C (Or immediately transfer to -20°C when done)

2.5.3 PCR Reaction

1). All primer stock solution should be diluted to 100 uM with 0.1 % DEPC H_2O. Then take 10 ul of forward primer, and 10 ul of reverse primer, add 80 ul of 0.1 % DEPC H_2O to make the 10 uM (FWD+REV) primer mix

2). Use 0.1 % DEPC H_2O to dilute the cDNA 10 times (10 ul of cDNA +90 ul of 0.1 % DEPC H_2O)

3). Vortex and spin down SYBR Green after thawing.

4). Set up the reaction in a thin-walled PCR tube on ice as below:

SYBR Green (2 X)	10 µl
Primer (FWD+REV) 10 uM	0.4 ul
cDNA (1:10)	2.0 ul
nuclease-free Water	7.6 µl
Total volume	20 µl

5). Perform qPCR using the recommended thermal cycling conditions.

Outlined below is the PCR program:

Step	Temperature, °C	Time	Number of cycles
Initial Denaturation	94	30 s	1
Denaturation	94	30 s	25-40 cycles
Annealing	Tm-5 (55~65)	30 s	
Extension	72	30s	
Final Extension	72	7min	1

2.5.4 Nucleotide sequences of primers used for quantitative real-time PCR

Gene Name	**Primer Sequence**
Hs-18S-Fwd	CGGCGACGACCCATTCGAAC
Hs-18S-Rev	GAATCGAACCCTGATTCCCCGTC
Hs-LDHA-Fwd	GGCTACAACAGGATTCTA
Hs-LDHA-Rev	TTACAAACCATTCTTATTTCTAAC
Hs-PKM2-Fwd	ATAACGCCTACATGGAAAAGTGT
Hs-PKM2-Rev	TAAGCCCATCATCCACGTAGA
Hs-PDK1-Fwd	ACCAGGACAGCCAATACAAG
Hs-PDK1-Rev	CCTCGGTCACTCATCTTCAC
Hs-Glut1-Fwd	CGGGCCAAGAGTGTGCTAAA
Hs-Glut1-Rev	TGACGATACCGGAGCCAATG
Hs-Glut2-Fwd	GCTGCTCAACTAATCACCATGC
Hs-Glut2-Rev	TGGTCCCAATTTTGAAAACCCC
Hs-Glut3-Fwd	GCTGGGCATCGTTGTTGGA
Hs-Glut3-Rev	GCACTTTGTAGGATAGCAGGAAG
Hs-Glut4-Fwd	ATCCTTGGACGATTCCTCATTGG
Hs-Glut4-Rev	CAGGTGAGTGGGAGCAATCT
Hs-PGK1-Fwd	GACCTAATGTCCAAAGCTGAGAA
Hs-PGK1-Rev	CAGCAGGTATGCCAGAAGCC
Hs-TPI1-Fwd	AAAGCTGGTGCCGTTGAGAA
Hs-TPI1-Rev	GGTTGTGGTAAACCTCTGCTC
Hs-PFKL-Fwd	GTACCTGGCGCTGGTATCTG

Hs-PFKL-Rev	CCTCTCACACATGAAGTTCTCC
Hs-SCD1-Fwd	AGAATGGAGGAGATAAGT
Hs-SCD1-Rev	TAGCAGAGACATAAGGAT
Hs-HK2-Fwd	CCAGTTCATTCACATCATCAG
Hs-HK2-Rev	CTTACACGAGGTCACATAGC
Hs-ENO1-Fwd	GCCGTGAACGAGAAGTCCTG
Hs-ENO1-Rev	ACGCCTGAAGAGACTCGGT
Hs-G6PD-Fwd	ACCGCATCGACCACTACCT
Hs-G6PD-Rev	TGGGGCCGAAGATCCTGTT
Hs-HIF-1α-Fwd	GAACGTCGAAAAGAAAAGTCTCG
Hs-HIF-1α-Rev	CCTTATCAAGATGCGAACTCACA

2.6 Protein extraction and SDS-PAGE (Western blotting)

1) Grow cells on 10 cm dishes.

2) Wash the plates twice with 10 ml of pre-cold 1 x PBS. Add 8ml of pre-cold PBS and scrape cells into 15 ml tube and then centrifuged at a speed of 3000 rpm for 5 minutes at 4°C. Remove the supernatant completely by spinning down again.

3) Add RIPA Buffer (50 mM Tris–HCl, pH 8.0, 150 mM NaCl, 5 mM EDTA, 0.1 % SDS, 1% NP-40, cocktail) to lyse the cells, and transfer the sample to pre-cooled EP tubes.

4) Sit on ice for 45~60 minutes, vortex 2-3 times during the incubation.

5) Protein lysates are centrifuged at 14,000 rpm for 10 minutes at 4°C.

6) Transfer the supernatant to new pre-cooled EP tubes.

7) Quantification of protein using the Bradford method by measuring OD595 using Spectrometer.

8) Use 5 x SDS buffer to adjust the concentration of protein and boil it for 5mins.

9) Load protein along with a pre-stained protein ladder marker.

10) The electrophoresis is performed at 80 v voltage. After the sample completely run out of the stacking gel, the voltage is adjusted to 120 v voltage and the separation continued for about 1 hour

11) Transfer for 1.5 ~ 2 hours per blot.

12) After the membrane transfer is completed, NC membrane or PVDF membrane was

blocked with 5 % Non-fat-dry milk (NFDM) within 1 x washing buffer for about 1 hour

13) Incubate membranes with primary antibody at indicated dilution for 1.5 hours, followed by washing with 1x washing buffer for 3 x 10 min

14) Incubate membranes with secondary antibody at indicated dilution for 1 hour, followed by washing with 1x washing buffer for 3 x 10 min

15) Remove the membrane and place it on saran wrap. Mix equal volumes of ECL reagents and evenly spread on NC membrane or PVDF membrane, and the membrane is placed in Chemiluminescence imaging instrument for developing following the manufactory instructions

2.7 Treatment model of mouse xenograft assay

4-week-old male BALB/c nude mice were injected with 5 x 10^6 Hep3B cells subcutaneously. At day 10, intragastric administration of Pteryxin with different concentrations (0.08 mg / kg，0.3 mg / kg，1.5 mg / kg) were performed every other day. corresponding doses of vehicle DMSO was administration as the control group. Tumor size was measured by vernier calipers every three days after administration. Calculation formula: tumor volume = width (mm) *depth (mm) *length (mm) *0.52. At day 26, the mice were weighed and the experiment was terminated. The tumor lysates were extracted, and the related protein levels were detected.

2.8 Prevention model of mouse xenograft assay

Intragastric administration of 0.08 mg / kg Pteryxin was performed in 4-week-old BALB/c nude mice every other day., corresponding doses of vehicle DMSO was administrated as the control group. 10 days later, 5 x 10^6 Hep3B cells are injected into the mice subcutaneously. Pteryxin was continuously given every other day. Tumor size was measured by vernier calipers at indicated time points after tumor inoculation. Calculation formula: tumor volume = width (mm) *depth (mm) *length (mm) *0.52. At day 30, the experiment was terminated and tumors are extracted.

2.9 Drug treatment and cell viability detection in organoid models

Clinical human liver cancer patient-derived organoids and normal liver-derived

organoids were digested into single cell with 0.25 % Trypsin-EDTA. After counting, organoids were suspended in 2 % matrigel/growth media and dispensed into BME (Basement Membrane Extract) coated 96-well plates at a density of 5000 cells per well. After 3 days, the medium was changed into fresh medium containing Pteryxin. The medium was changed every 3 days. The organoids were treated with Pteryxin for 6 days. After 6 days of drug treatment, CellTiter-Glo® 3D Reagent was added to each well. Mix the contents vigorously for 5 minutes to induce cell lysis. Allow the plate to incubate at room temperature for an additional 25 minutes to stabilize the luminescent signal. Luminescence was measured on a Synergy H1 Multi-Mode Reader. Results were compared to the control group (DMSO) and curve fitting was performed according to Prism (GraphPad) software and the nonlinear regression equation. Photographs of organoids treated with DMSO, 50 uM or 100 uM pteryxin for 6 Days in 24-well plates were collected by optical microscope under white light and 10x objective field conditions.

For qRT-PCR assay, digested organoid was re-suspended with BME into 6-well plate, then these organoids were treated with DMSO, 50 uM or 100 uM pteryxin under normoxic or hypoxic conditions for 48 hours, respectively. RNA was extracted by (Magen R4111-02) Hipure total RNA mini kit. Reverse transcription and the following methods are the same as mentioned in “2.5 Total RNA extraction and qRT-PCR”.

3. Results

3.1 Pteryxin suppresses the proliferation of hepatocellular carcinoma cells, especially under hypoxic conditions

To screen for potential herbal extracts with anti-cancer effect, we purchased a library including 29 herbal extracts and examined their inhibitory effect on Hep3B liver cancer cells. It is interesting to find that after 96 hours treatment, hepatocellular carcinoma cell numbers decreased significantly by Wogonin, Cryptotanshinone, Tanshinone I, Tanshinone IIA, Pteryxin and Palmatine chloride at dose of 100 uM (**Figure 1A**). While the anti-tumor effects for some compounds have been reported [11-15], there is no previous report documenting whether and how Pteryxin suppresses tumor cell proliferation. Therefore, we

focused on the inhibitory effect of Pteryxin and explored the potential molecular mechanism.

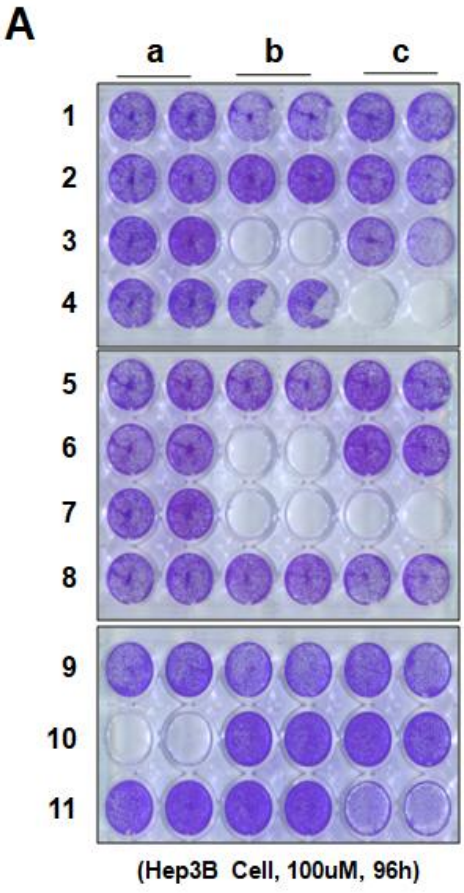

Rank	Name	Chinese Name	Antitumor Effect	Remark (about antitumor effect)
1b	Baicalein	黄芩素	+	
1c	Malic acid	苹果酸	-	
2a	Scutellarein	野黄芩素	-	
2b	Scutellarin	野黄芩苷	-	
2c	Baicalin	黄芩苷	-	
3a	Wogonoside	次黄芩苷	-	
3b	Wogonin	次黄芩素	+++	Known
3c	Cycloastragenol	环黄芪醇	+	
4a	AstragalosideIV	黄芪甲苷	-	
4b	AstragalosideIII	黄芪皂苷III	-	
5b	Tanshinone IIA-sulfonic sodium	丹参酮IIA磺酸钠	-	
5c	Sodium Danshensu	丹参素钠	-	
6a	Calycosin	毛蕊异黄酮	-	
6b	Cryptotanshinone	隐丹参酮	+++	Known
6c	Salvianolic acid B	丹酚酸B	-	
7a	Salvianolic Acid C	丹酚酸C	-	
7b	Tanshinone I	丹参酮I	+++	Known
7c	Tanshinone IIA	丹参酮IIA	+++	Known
8a	Dihydrotanshinone I	二氢丹参酮I	-	
8b	Paeonol	芍药醇	-	
8c	Protocatechuic acid	原儿茶酸	-	
9b	Protocatechualdehyde	原儿茶醛	-	
9c	D-Mannitol	甘露醇	-	
10a	(+)-Pteryxin	北美芹素	+++	Unknown
10b	Allitol	蒜糖醇	-	
10c	4-Hydroxybenzyl alcohol	对羟基苯甲醇	-	
11a	Tubuloside A	管花苷A	-	
11b	Cordycepin	虫草素	-	
11c	Palmatine chloride	盐酸巴马汀	++	Known

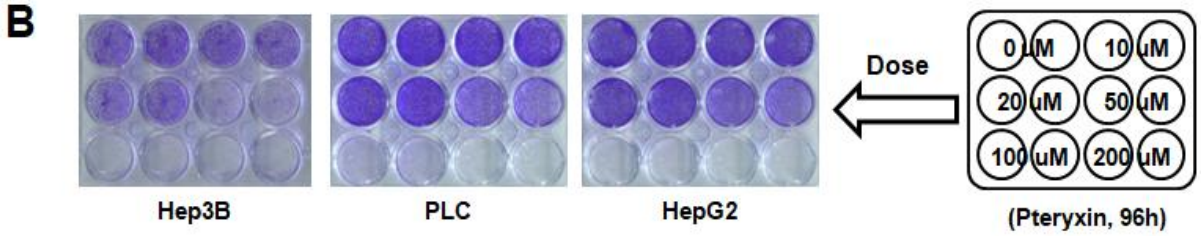

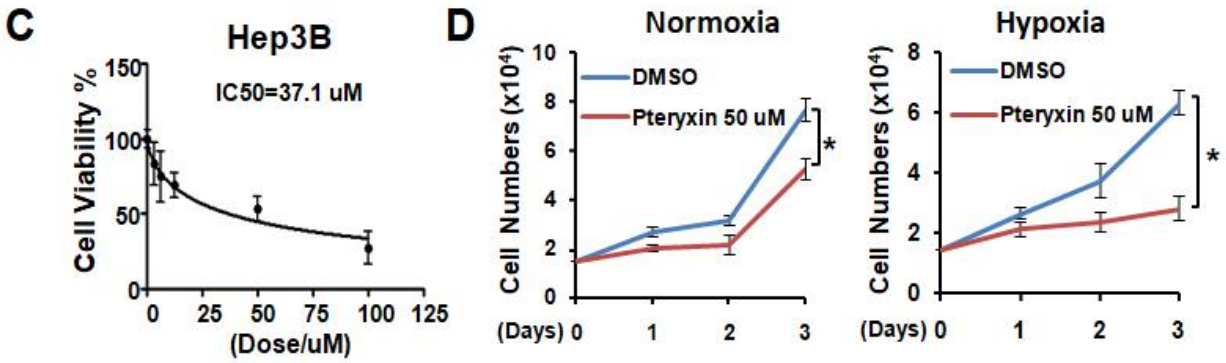

Figure 1: Pteryxin suppresses hepatocellular carcinoma cell proliferation, especially under hypoxic conditions. (**A**) Crystal violet assay was performed in Hep3B cells treated with 29

kinds of natural compound (100 uM) for 96 hours (left panel). The table shows the anti-tumor effect of each compound in the screening assay (right panel). The wells of 1a, 5a, and 9a were DMSO control groups and the wells of 4c were blank controls. (**B**) Crystal violet assay was performed in Hep3B, PLC and HepG2 cells treated with 0 uM, 20 uM, 50 uM, 100 uM, or 200 uM of Pteryxin for 96 hours. (**C**) Cell viability of Hep3B cells was tested by MTT assay after treatment with Pteryxin for 48 hours, IC50 was calculated. (**D**) Growth curves of Hep3B cells treated with 50 uM Pteryxin under normoxia and hypoxia were determined by trypan blue counting, respectively. *P < 0.05 by Student's *t*-test.

In order to explore whether the inhibitory effect of Pteryxin is common in cancer cells and its dose dependency, Hep3B, PLC and HepG2 hepatocellular carcinoma cancer cells were treated with 10 uM, 20 uM, 50 uM, 100 uM, and 200 uM of Pteryxin for 96 hours. Results showed that Pteryxin inhibited cell proliferation in all these liver cancer cell lines in a dose-dependent manner, with 50 uM Pteryxin partially inhibiting cell proliferation and 100 uM Pteryxin completely killing these cells (**Figure 1B**). By MTT assay, we found that the IC50 of Pteryxin in Hep3B cells is 37.1 uM (**Figure 1C**). Since hypoxia is an important microenvironment for solid tumors including liver cancer, Hep3B cells were treated with 50 uM Pteryxin under normoxic or hypoxic conditions, respectively. Cell growth curve analysis revealed that the inhibitory effect of Pteryxin was more potent under hypoxic conditions compared to normoxic conditions, though Pteryxin could inhibit cell proliferation under both conditions (**Figure 1D**). In brief, Pteryxin inhibits the proliferation of liver cancer cells and has more potent inhibitory effect under hypoxic conditions.

3.2 Pteryxin inhibits the expression of glucose metabolic enzymes induced under hypoxia

Due to the potent anti-tumor effect of Pteryxin under hypoxic conditions, we next investigated the potential mechanism under hypoxia. We treated Hep3B cells with normoxic condition, hypoxic and hypoxic condition with Pteryxin treatment for 24 hours, then collected RNA for RNA-seq analysis. The results showed that 604 genes were up-regulated by 1.5 fold under hypoxic condition compared to normoxic condition, 3071 genes were up-regulated by 1.5 fold under hypoxic condition compared to hypoxic condition with Pteryxin treatment. Among them, 392 genes were co-upregulated in both cases by 1.5 fold (**Figure 2A**). Further gene ontology (GO) term enrichment analysis (DAVID:

https://david.ncifcrf.gov/) showed that these 392 genes are enriched in glucose metabolism (including genes of glycolysis and gluconeogenesis) and hypoxia response (**Figure 2B**).

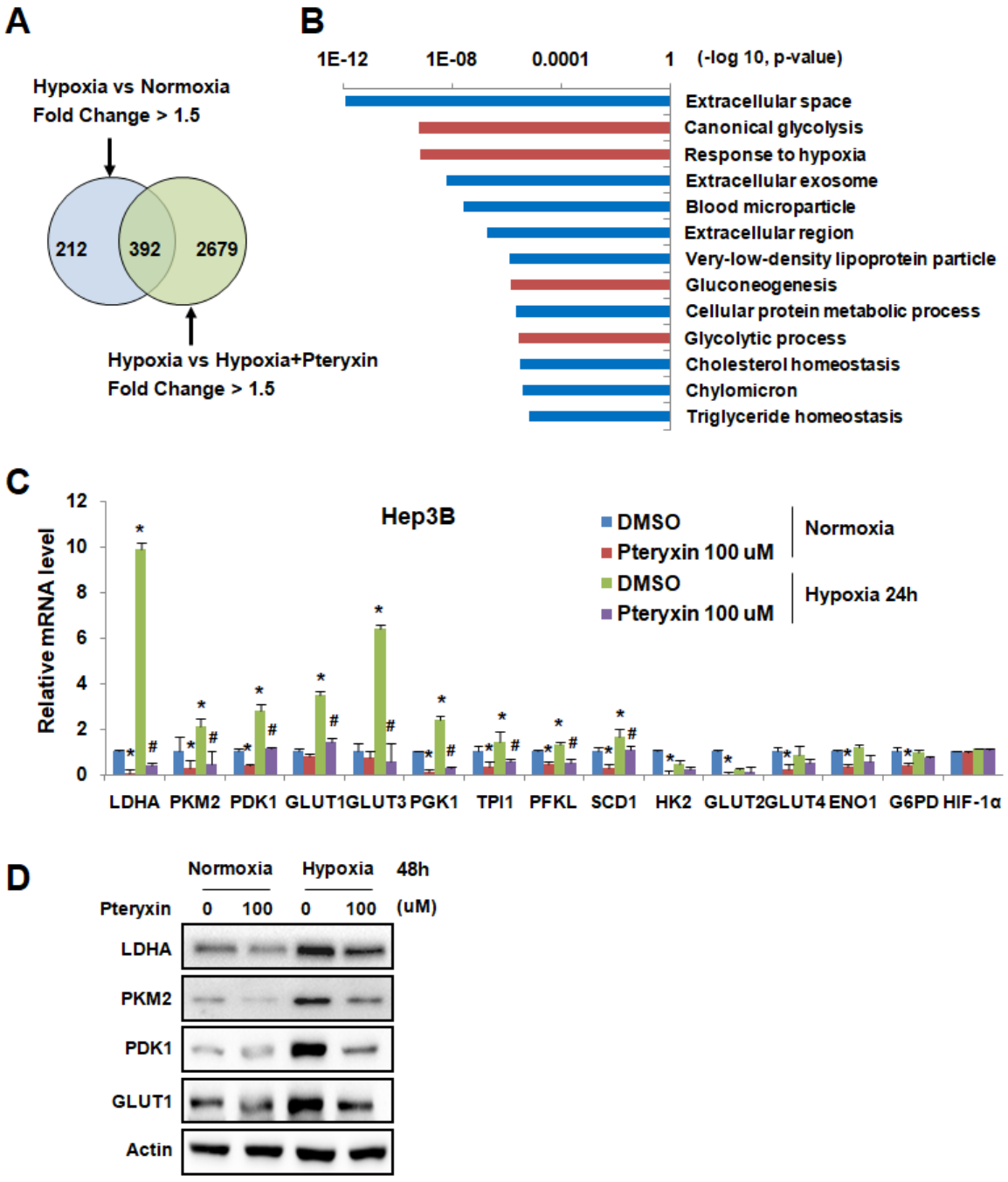

Figure 2: Pteryxin inhibits the expression of glucose metabolic enzymes induced under hypoxia. (**A**) Venn diagram showing overlapping of the up-regulated genes in the hypoxic condition compared to normoxic condition or compared to the group with 100 uM Pteryxin treatment under hypoxic conditions based on the RNA-Seq data. (**B**) Analysis of 392 overlapping genes by Gene Ontology (GO) term enrichment. (**C**, **D**) qRT-PCR (**C**) and Western blotting (**D**) analysis of the expression of glycolytic enzymes in Hep3B cells cultured under normoxic or hypoxic conditions for 24 hours or 48 hours in the presence of DMSO or 100 uM Pteryxin, respectively. *P < 0.05 as compared to normoxic DMSO group,

$^{\#}P < 0.05$ as compared to hypoxic DMSO group by Student's *t*-test.

Next, Hep3B cells were treated with 100 uM Pteryxin for 24 hours to detect the mRNA expression of glucose metabolic enzymes under normoxic or hypoxic conditions. We found that Pteryxin remarkably inhibited the hypoxia-induced expression of lactate dehydrogenase A (LDHA), pyruvate kinase M2 (PKM2), pyruvate dehydrogenase kinase isoenzyme 1 (PDK1), Glucose transporter 1 (GLUT1), phosphoglyceric kinase 1 (PGK1) (**Figure 2C**). Under the same conditions, Hep3B cells were treated for 48 hours and protein samples were collected and detected by Western blotting. The data showed that, consistent with the mRNA results, Pteryxin markedly suppressed the protein levels of hypoxia triggered accumulation of glucose metabolic enzymes such as LDHA, PKM2, PDK1 and Gult1 (**Figure 2D**). Collectively, Pteryxin inhibits the expression of glucose metabolic enzymes at both mRNA and protein levels under hypoxic conditions.

3.3 Pteryxin inhibits the expression of HIF1α protein

Results in Figure 2 indicate that Pteryxin regulates the enzyme of glucose metabolism at the transcriptional level. It is known that HIF-1, as an important transcription factor, extensively regulates the transcription of enzymes involved in glucose metabolism under hypoxic conditions. However, it is unknown whether Pteryxin regulates glucose metabolism via HIF-1α. Based on this speculation, we examined the protein expression of HIF-1α in Hep3B cells treated with 50 uM Pteryxin for 6 hours under normoxic and hypoxic conditions, respectively. Western blotting results revealed that Pteryxin markedly inhibited the accumulation of HIF-1α protein under hypoxic conditions (**Figure 3A**). Furthermore, Hep3B cells were treated with 50 uM or 100 uM Pteryxin in the presence of hypoxia mimics cobalt chloride (CoCl2), desferrioxamine (DFX), dimethyloxalylglycine (DMOG) or proteasome inhibitor MG-132 for 6 hours. Western blotting results showed that Pteryxin dose-dependently inhibited the protein expression of HIF-1α, even in the presence of the hypoxia mimics or MG-132. (**Figure 3B**). Figure 2C and 3B indicated that Pteryxin didn't inhibit the mRNA expression and protein degradation of HIF-1α, therefore, it is possible that Pteryxin may affect HIF-1α protein translation.

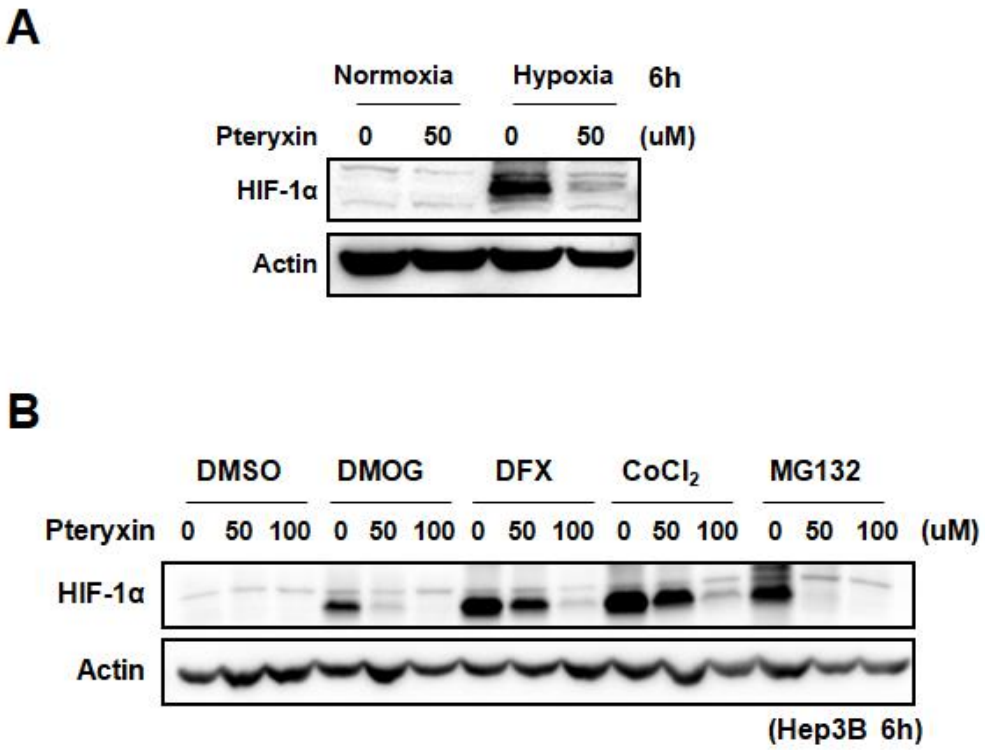

Figure 3: Pteryxin inhibits HIF-1α protein expression. (**A**) Hep3B cells were exposed to DMSO or 50 uM of Pteryxin for 6 hours under normoxic or hypoxic conditions and whole-cell lysates were subjected to Western blotting analysis of HIF-1α protein. Actin served as loading control. (**B**) Hep3B cells were exposed to DMSO or 0, 50 or 100 uM Pteryxin in the presence of the hypoxia mimics cobalt chloride ($CoCl_2$), desferrioxamine (DFX), dimethyloxalylglycine (DMOG) or proteasome inhibitor MG-132 for 6 hours and whole-cell lysates were subjected to Western blotting analysis of HIF-1α protein. Actin served as loading control.

3.4 Pteryxin inhibits hepatocellular carcinoma progression in mouse tumor treatment models

The cell-based experiments data showed that Pteryxin significantly inhibited the proliferation of liver cancer cells under hypoxic conditions and suppressed HIF-1α as well as hypoxia-activated glucose metabolic enzymes. Since HIF-1α and these glucose metabolic enzymes are important for tumor cell growth especially under hypoxic conditions, next, we investigated the effect of Pteryxin in mouse tumor models. 5 x 10^6 Hep3B liver cancer cells were injected subcutaneously into mice to set up mouse xenograft models. When tumor volume reached the size about 100 mm^3, we randomly divided the mice into 4 groups and

DMSO, 0.08 mg/kg, 0.3 mg/kg or 1.5 mg/kg Pteryxin was given to each group of mice, respectively, by intragastric administration every other day. After treatment for 26 days, the experiment was terminated. As a results, the xenograft experiment in nude mice showed that Pteryxin significantly decelerated tumor growth in a dose-dependent manner (**Figur 4A**). Interestingly, Pteryxin treatment even completely blocked the tumor growth in some mice, especially for high dose treatment group, as shown in the tumor photograph (**Figure 4B**). Mouse bodyweight measurment showed no siginificant differences between these groups, suggesting the potenial of Pteryxin as an effective anti-cancer drug with no obvious side-effects (**Figure 4C**). Moreover, protein lysates of the tumor tissues were extracted and Western blotting confirmed that Pteryxin inhibited the protein expression of HIF-1α, PKM2, PDK1 and LDHA in mouse models (**Figure 4D**). Taken together, the results of mouse xenograft experiments indicate that Pteryxin inhibits liver cancer progression by suppressing HIF-1α as well as glucose metabolism *in vivo*.

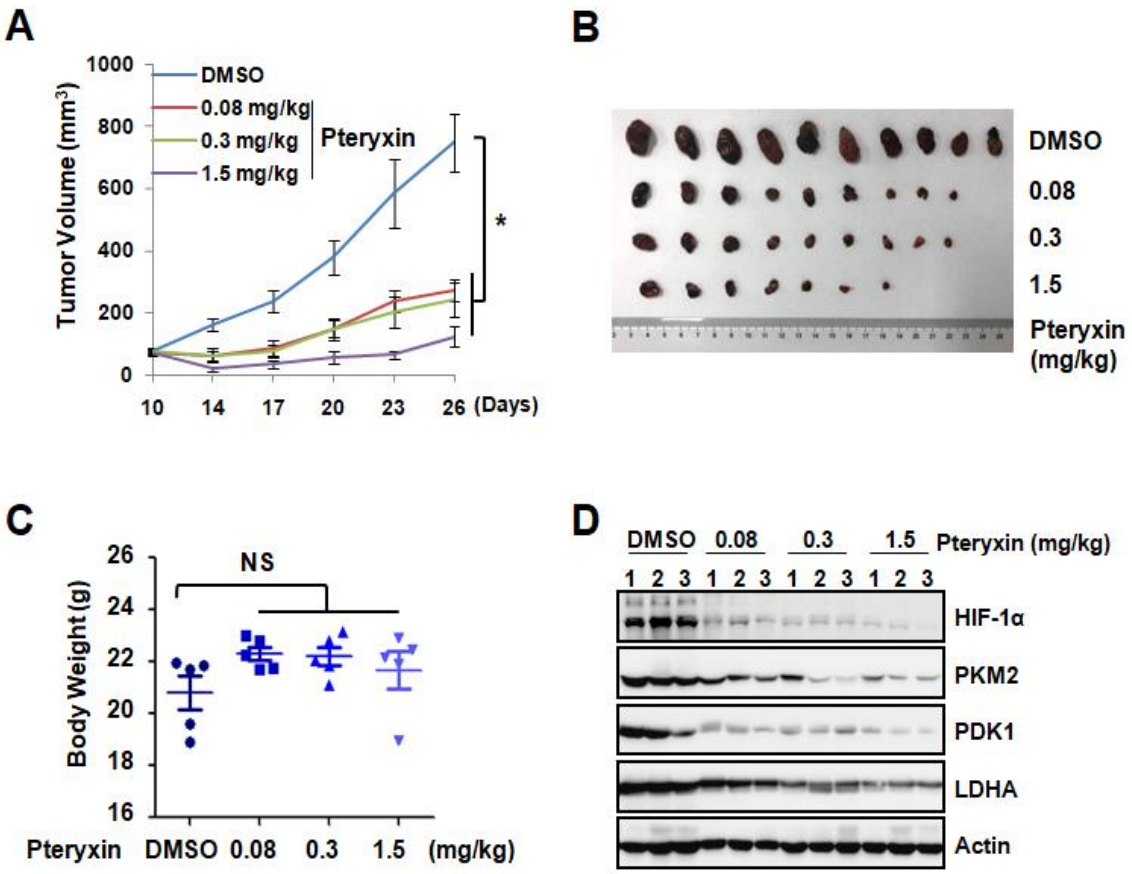

Figure 4: Pteryxin inhibits hepatocellular carcinoma progression in mouse tumor models. Hep3B cells were injected subcutaneously into nude mice. When tumor volume reached the size about 100 mm^3, mice were administered with DMSO, 0.08mg/kg, 0.3mg/kg or 1.5mg/kg Pteryxin by gavage every other day. n=5 for each group. (**A**) Tumor growth curves were measured starting from 10 days after inoculation. Data were presented as mean ± SEM. *P < 0.05 compared between the indicated groups by Student's *t*-test. (**B**) Photographs showed the size of the xenografts at the end of the experiment (**B**). (**C**) Mouse bodyweight was measured at the end of the experiment. (**D**) At the end of the experiment, tumors were extracted followed by Western blotting analysis of the expression of HIF-1α and indicated glycolytic enzymes. Actin served as loading control.

3.5 Pteryxin inhibits tumor initiation in mouse tumor prevention models

Next, we investigated whether Pteryxin could prevent tumorigenesis in another mouse tumor prevention model. We pretreated the mice with a low concentration of Pteryxin (0.08 mg/kg) by intragastric administration every other day and then injected tumor cells into the mice 10 days later. In the earlier stage, we found that Pteryxin delayed tumor development and that mice with Pteryxin pre-treatment had smaller tumors. After about 30 days, the experiment was terminated. As a result, tumor volume in Pteryxin treated group was much smaller compared with the control group (**Figure 5A, 5B**). Considering this is a tumor prevention model, this results demonstrate that Pteryxin prevents liver cancer initiation, suggesting its potential use as a kind of supplementation for tumor prevention in the future.

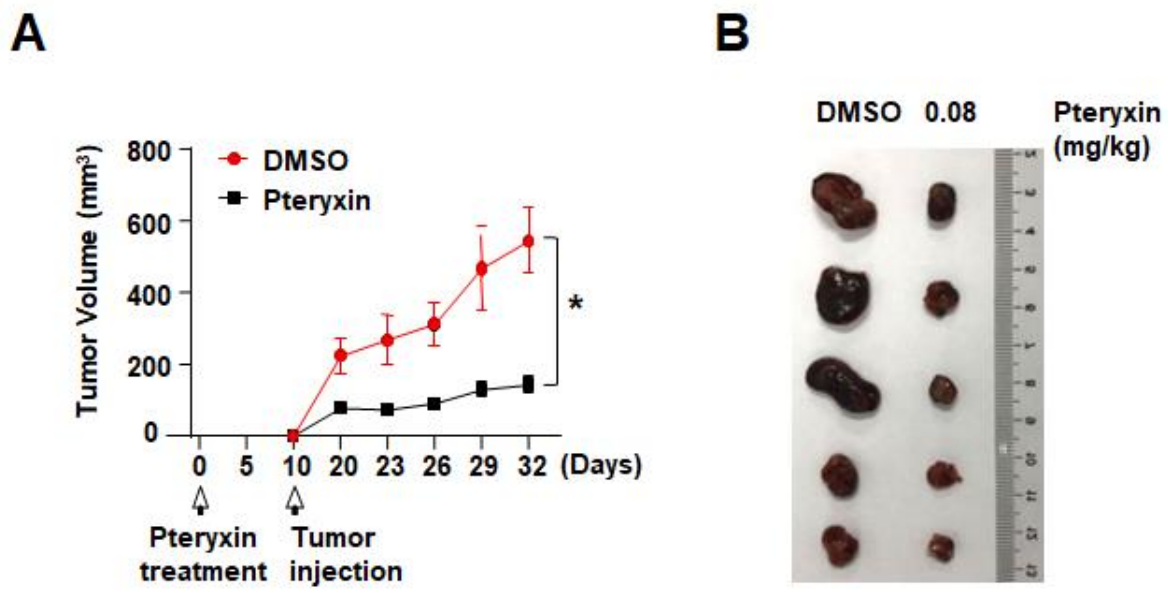

Figure 5: Pteryxin inhibits tumor initiation in mouse tumor prevention models. (**A**) Mice were administered with DMSO or 0.08mg/kg Pteryxin for 10 days by gavage every other day, 10 days later, Hep3B cells were injected subcutaneously into nude mice (n=5 for each group). Pteryxin was continuously given every other day after the tumor inoculation. Tumor growth curves were measured starting from inoculation. Data were presented as mean ± SEM. *P < 0.05 compared between the indicated groups by Student's *t*-test. (**B**) Photographs showed tumor xenografts at the end of the experiment.

3.6 Pteryxin suppresses the growth and glycolytic enzymes in hepatocellular carcinoma patient-derived organoids

Organoid is a three-dimensional micro-organ culture model developed on the basis of cell culture in culture dishes. It highly mimics the source tissues and organs and can help us better evaluate the function of drugs [16-17]. Here, we used clinical hepatocellular carcinoma patient-derived tumor organiods and normal human liver-derived organiods to examine the tumor-killing effect and evaluate side-effect of Pteryxin. By using MTT assay, we found that IC50 of Pteryxin in liver cancer patient-derived tumor organiods was 49.33 uM, much less than 103 uM, the IC50 of Pteryxin in normal liver-derived organiods (**Figure 6A**). The data indicated that low dose of Pteryxin could efficiently suppress the growth of liver cancer patient-derived tumor organiods, but with little effects on normal liver-derived organoids. This speculation was confirmed by direct observation from the microscope, 50 uM or 100 uM Pteryxin obviously inhibited the proliferation of liver cancer patient-derived tumor organiods, but 50 uM Pteryxin exhibited no, while 100 uM Pteryxin exhibited marginal effects on the proliferation of normal liver-derived organiods (**Figure 6B**). Furthermore, mRNA expressions of glucose metabolic enzymes were detected in liver cancer patient-derived tumor organoids treated with 50 uM or 100 uM Pteryxin under normoxic or hypoxic conditions for 48 hours, respectively. Consistent with the cell line-based results, Pteryxin inhibited the mRNA expressions of the hypoxia-induced glucose metabolic enzymes in the organoid models (**Figure 6C**). Thus, Pteryxin inhibits the growth of hepatocellular carcinoma patient-derived tumor organiods and glucose metabolic enzymes, suggesting its high clinical application potential for anti-tumor therapy.

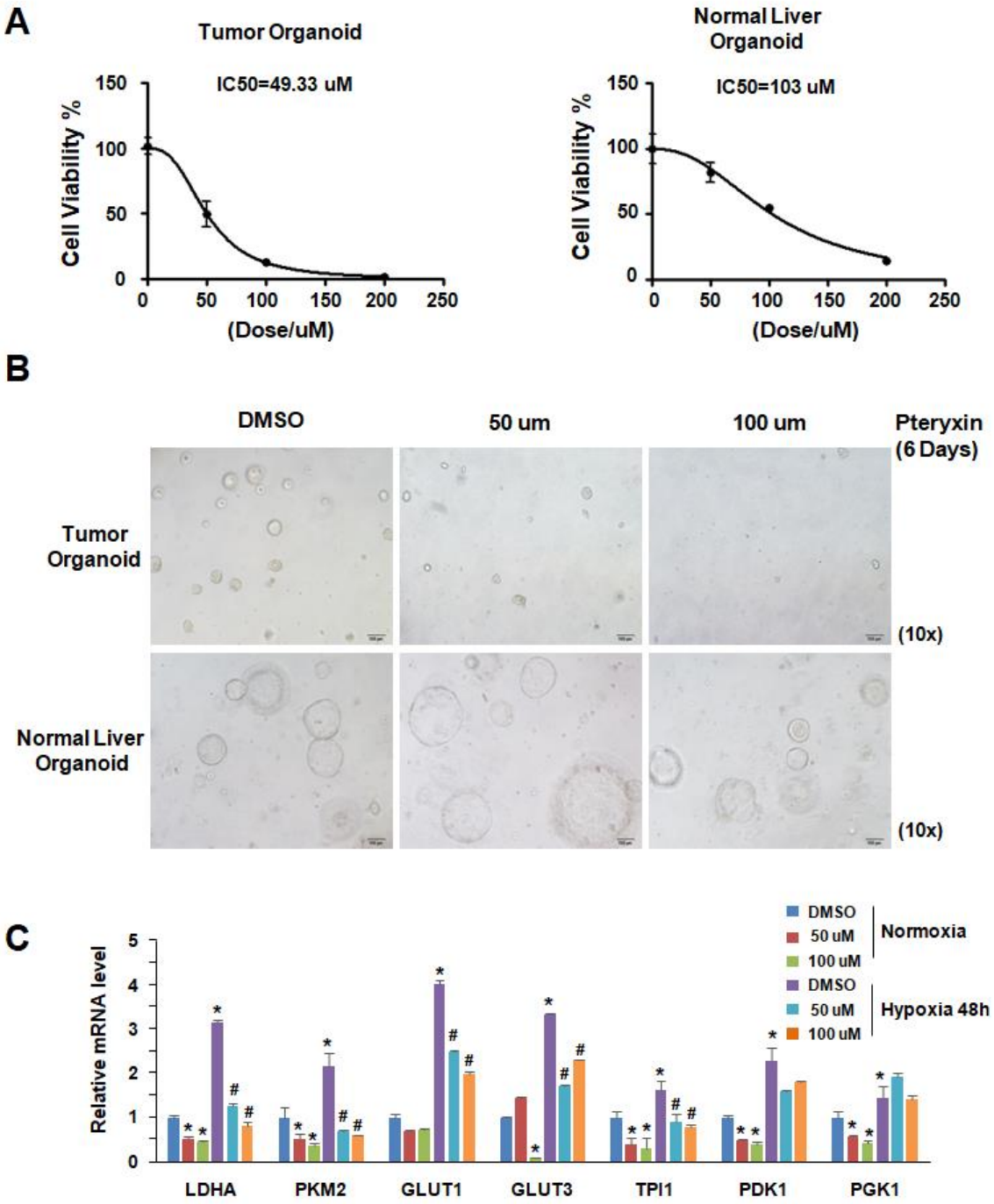

Figure 6: Pteryxin suppresses the growth and glycolytic enzymes expression in human hepatocellular carcinoma patient-derived organoids. (**A**) Cell viability was measured in human liver cancer patient-derived tumor organoids and normal liver-derived organoids treated with DMSO, 50 uM, 100 uM, or 200 uM Pteryxin for 6 days, respectively, IC50 was calculated. (**B**) Representative bright field images of human liver cancer patient-derived tumor organoids and normal liver-derived organoids treated with DMSO, 50 uM, or 100 uM Pteryxin for 6 days, respectively. Scale bar: 100 um. (**C**) qRT-PCR analysis of the glycolytic enzymes in human liver cancer patent-derived tumor organoids cultured under normoxic or hypoxic conditions for 48 hours in the presence of DMSO, 50 uM or 100 uM Pteryxin, respectively.

4. Conclusions and Perspectives

Through the screening of a series of compounds from Chinese herbal medicines, our study found that Pteryxin could inhibit the proliferation of hepatocellular carcinoma cells and that its inhibitory effect was more potent under hypoxic conditions. RNA-seq analysis and subsequent experiments showed that Pteryxin suppressed the expression of HIF-1α and the hypoxia-induced activation of glucose metabolic enzymes. Treatment and prevention models of mouse xenograft experiments revealed that Pteryxin decelerated liver cancer tumorigenesis and progression by inhibiting HIF-1α and glucose metabolism, without affecting mouse bodyweight. Similar results were obtained in the tumor organoid models derived from clinical hepatocellular carcinoma patients. Taken together, Pteryxin inhibits liver cancer cell proliferation, suppresses liver cancer tumorigenesis and progression in mouse xenografts and clinical cancer patient-derived tumor organoid models both *in vitro* and *in vivo*. In conclusion, these results indicate that Pteryxin is a potential herbal compound for anti-cancer therapy, and holds great potential and significance for cancer prevention as well as cancer treatment.

Nowadays, there is no perfect therapy for cancer patients, especially for the solid tumor patients. Development of new and effective anti-tumor drugs is still the top priority. After thousands of years of use, traditional Chinese medicine has been shown to be effective in cancer treatment, but the effective ingredients and potential anti-cancer mechanisms of most traditional Chinese medicine are still far from clear. Thus, the screening out of Pteryxin as a potential anti-tumor drug is of great significance. Previous reports have examined the pharmacokinetics of Pteryxin, and found that Pteryxin prevents obesity and inflammation, but the effects of Pteryxin on cancer are still largely unknown. By adopting multiple models, we demonstrated the cancer prevention and therapeutic effects of Pteryxin both *in vitro* and *in vivo*. Potential mechanism study revealed that the inhibitory effect of Pteryxin on cancer was achieved by targeting HIF-1α and glucose metabolism. Considering the fact that Pteryxin is easy to be ingested and beneficial to individual organisms, exploring its function in cancer prevention and treatment is very promising and holds great potential.

Systematical exploration of the specific molecular mechanism underlying the

anti-cancer effect of Pteryxin warrants further investigation. It is also worth exploring whether it is effective in other types of cancer. In addition, more efforts should be employed to study whether it can be further optimized, developed and combined with other treatments such as immunotherapy to prevent and treat cancers.

5. Acknowledgement

This thesis was completed under the guidance and organization of Dr. Linchong Sun from the School of Medicine, South China University of Technology. Over the past two years, Dr. Sun has devoted tremendous efforts to supervising me with this study. Meanwhile, I would like to thank Rui Chen, Hui Lu, Zhiyuan Lin, Yang Zhang and other students from Dr. Sun′s group for their help with the experimental operation and data analysis. I learned a lot from them. Thank Novogene Company (Beijing, China) for providing the RNA sequencing data. This is a great experience for me. I have truly enjoyed the fun of doing research. Meanwhile, I also deeply appreciated the importance of perseverance and determination in doing scientific research. Thank all the people for their helps and suggestions during this study.

6. Reference

1. Matsuda, H., Murakami, T., Kageura, T., Ninomiya, K., Toguchida, I., Nishida, N., and Yoshikawa, M. (1998). Hepatoprotective and nitric oxide production inhibitory activities of coumarin and polyacetylene constituents from the roots of Angelica furcijuga. Bioorganic & medicinal chemistry letters *8*, 2191-2196.
2. Nugara, R.N., Inafuku, M., Takara, K., Iwasaki, H., and Oku, H. (2014). Pteryxin: a coumarin in Peucedanum japonicum Thunb leaves exerts antiobesity activity through modulation of adipogenic gene network. Nutrition (Burbank, Los Angeles County, Calif) *30*, 1177-1184.
3. Yoshikawa, M., Nishida, N., Ninomiya, K., Ohgushi, T., Kubo, M., Morikawa, T., and Matsuda, H. (2006). Inhibitory effects of coumarin and acetylene constituents from the roots of Angelica furcijuga on D-galactosamine/lipopolysaccharide-induced liver injury in mice and on nitric oxide production in lipopolysaccharide-activated mouse peritoneal macrophages. Bioorganic & medicinal chemistry *14*, 456-463.

4. Nugara, R.N., Inafuku, M., Takara, K., Iwasaki, H., and Oku, H. (2014). Pteryxin: a coumarin in Peucedanum japonicum Thunb leaves exerts antiobesity activity through modulation of adipogenic gene network. Nutrition (Burbank, Los Angeles County, Calif) *30*, 1177-1184.
5. Wang, J., Ma, Y., Li, W., Hu, F., Chen, T., Shen, X., and Feng, S. (2012). Study on pharmacokinetics and tissue distribution of pteryxin in mice by ultra-pressure liquid chromatography with tandem mass spectrometry. Biomedical chromatography : BMC 26, 802-807.
6. 柏连阳，陈桂华，刘二明，et al. 北美芹素在诱导水稻抗稻瘟病和抗寒性中的应用：CN. CN101766172 B.
7. Semenza, G.L. (2003). Targeting HIF-1 for cancer therapy. Nature reviews Cancer *3*, 721-732.
8. Majmundar, A.J., Wong, W.J., and Simon, M.C. (2010). Hypoxia-inducible factors and the response to hypoxic stress. Molecular cell *40*, 294-309.
9. Vander Heiden, M.G., Cantley, L.C., and Thompson, C.B. (2009). Understanding the Warburg effect: the metabolic requirements of cell proliferation. Science (New York, NY) *324*, 1029-1033.
10. Koppenol, W.H., Bounds, P.L., and Dang, C.V. (2011). Otto Warburg's contributions to current concepts of cancer metabolism. Nature reviews Cancer *11*, 325-337.
11. Li-Weber, M. (2009). New therapeutic aspects of flavones: the anticancer properties of Scutellaria and its main active constituents Wogonin, Baicalein and Baicalin. Cancer treatment reviews *35*, 57-68.
12. Shin, D.S., Kim, H.N., Shin, K.D., Yoon, Y.J., Kim, S.J., Han, D.C., and Kwon, B.M. (2009). Cryptotanshinone inhibits constitutive signal transducer and activator of transcription 3 function through blocking the dimerization in DU145 prostate cancer cells. Cancer research *69*, 193-202.
13. Lee, C.Y., Sher, H.F., Chen, H.W., Liu, C.C., Chen, C.H., Lin, C.S., Yang, P.C., Tsay, H.S., and Chen, J.J. (2008). Anticancer effects of tanshinone I in human non-small cell lung cancer. Molecular cancer therapeutics *7*, 3527-3538.
14. Chiu, T.L., and Su, C.C. (2010). Tanshinone IIA induces apoptosis in human lung cancer A549 cells through the induction of reactive oxygen species and decreasing the mitochondrial membrane potential. International journal of molecular medicine *25*, 231-236.
15. Zhang, L., Li, J., Ma, F., Yao, S., Li, N., Wang, J., Wang, Y., Wang, X., and Yao, Q. (2012). Synthesis and cytotoxicity evaluation of 13-n-alkyl berberine and palmatine analogues as anticancer agents. Molecules (Basel, Switzerland) *17*, 11294-11302.

16. Sun, L., Wang, Y et al. (2019). Modelling liver cancer initiation with organoids derived from directly reprogrammed human hepatocytes. Nature Cell Biology *21*, 1015-1026.
17. Broutier, L., Mastrogiovanni, G., Verstegen, M.M., Francies, H.E., Gavarro, L.M., Bradshaw, C.R., Allen, G.E., Arnes-Benito, R., Sidorova, O., Gaspersz, M.P.*, et al.* (2017). Human primary liver cancer-derived organoid cultures for disease modeling and drug screening. Nature Medicinec *23*, 1424-1435.

题目：北美芹素通过靶向 HIF-1α 及糖代谢抑制肝癌的发生发展

参赛队员：王越洋

（华南师范大学附属中学 国际部）

指导老师： 孙林冲 博士

（华南理工大学医学院副教授、研究生导师）

地区：广东省广州市

华南师范大学附属中学国际部
International Department, The Affiliated High School of SCNU

目 录

北美芹素通过靶向 HIF-1α 及糖代谢抑制肝癌的发生发展

王越洋 华南师范大学附属中学 国际部

摘要

从中草药化合物中开发新型抗肿瘤药物是目前肿瘤治疗领域的一大特色。通过一系列中草药来源化合物的筛选，我们发现白花前胡提取物北美芹素具有显著的抗癌效果。在体外细胞水平，北美芹素可抑制多种肝癌细胞的增殖，并且这种抑制效果在低氧微环境条件下更为显著。初步机制研究表明，北美芹素可以在蛋白水平抑制低氧诱导因子 1α（HIF-1α）的表达，并进而下调受 HIF-1α 转录调控的多种葡萄糖代谢酶的表达，达到抑制细胞增殖的效果。进一步体内移植瘤实验发现，在小鼠肿瘤治疗和预防模型中，北美芹素均可显著抑制小鼠肝癌的发生和发展且无明显的毒副作用。最后，利用临床肝癌病人样本所建立的肝癌类器官模型，我们发现低浓度的北美芹素可下调低氧条件下激活的葡萄糖代谢酶的表达并显著抑制肝癌组织来源的类器官生长，但对正常肝脏组织来源的类器官无明显影响。

综上所述，我们发现北美芹素可以在不同模型中有效抑制肝癌的发生发展，为肿瘤的预防和治疗提供新靶向药物的同时，对中草药化合物的推广和临床应用也具有重要意义。

关键词：中草药 北美芹素 肝癌 低氧 葡萄糖代谢

Pteryxin suppresses hepatocellular carcinoma by targeting HIF-1α and glucose metabolism

Yueyang Wang, International Department of the Affiliated High School of South China Normal University

Abstract

The development of new anti-cancer drugs from Chinese herbal compounds is drawing much attention in the field of cancer therapy. In this study, we performed a small scale drug screening to identify potential anti-cancer herbal compounds. As a result, we found that Pteryxin, extracted from the plant *Peucedanum praeruptorum Dunn*, exhibited strong anti-tumor effects. Pteryxin inhibits cell proliferation in multiple hepatocellular carcinoma cell lines, including Hep3B, HepG2 and PLC. More interestingly, this inhibitory effect is much more potent under hypoxic conditions. Mechanistic analysis revealed that Pteryxin suppresses the expression of HIF-1α (hypoxia-inducible factor 1α) at protein level as well as the expression of glucose metabolic enzymes at both mRNA and protein levels, suggesting that Pteryxin suppresses HIF-1α-mediated glucose metabolism. Moreover, mice xenograft experiments showed that Pteryxin efficiently prevented tumor initiation and inhibited tumor progression *in vivo*. Importantly, Pteryxin markedly inhibited the proliferation of clinical human liver cancer patient-derived organoids by targeting glucose metabolism, with marginal effect on the normal liver-derived organoids, indicating its specific toxic effect on tumor tissues and high anti-cancer implication potentials.

Collectively, Pteryxin efficiently suppresses liver cancer progression by inhibiting HIF-1α and hypoxia-activated glucose metabolism both *in vitro* and *in vivo*, presenting a new potential herbal compound for tumor prevention and anti-cancer therapy. Thus, the potential for the clinical application of our Chinese herbal compound, Pteryxin, warrants further study.

Key Words: Chinese herbal medicines, Pteryxin, hepatocellular carcinoma, hypoxia, glucose metabolism

声明

本人声明所提交的论文是在指导老师的悉心指导下进行的研究工作和取得的研究成果。据本人所知，除了文中特别加以标注和致谢中所罗列的内容以外，论文中不包含已经发表或正在投稿的研究成果。若有不实之处，本人愿意承担相关责任。

参赛队员签名：王越洋

日期： 2019 年 9 月 12 日

1. 引言 （研究背景及目标）

恶性肿瘤是威胁人类健康的常见疾病，占所有疾病致死率的四分之一。鉴于西药抗肿瘤的毒副作用及其治疗效果的局限性，从中草药中获取有效提取物进行肿瘤靶向治疗的研究已经成为肿瘤治疗领域的一大特色。中药是我国的瑰宝和国粹，也是未来开发治疗多种疾病的新型药物的重要来源，但是中成药纳入西方处方药尚需时日，且一些中成药抗肿瘤的机制还远未明了。因此，我们有必要寻找有效抗癌的中草药成分并探究其具体分子机制，以便进行进一步的临床试验和后续深入研究。

北美芹素（普里克生）是一种中草药的有效提取物，其主要来源于分布在我国西南部省份如四川、贵州、广西等地的伞形科植物白花前胡（*Peucedanum praeruptorum Dunn*）和竹叶西风芹（*Seseli mairei*）[1-2]。早期研究发现北美芹素可以抑制脂多糖（LPS）诱导的小鼠腹腔来源巨噬细胞一氧化氮的产生，从而发挥抗炎作用[3]。Nugara *et al.*发现北美芹素可以通过下调脂肪从头合成基因并上调脂肪分解基因而发挥抗肥胖作用，被认为是潜在的减肥药[4]。在小鼠模型中，北美芹素的药代动力学和组织分布研究表明其被口服后，可通过循环系统进入小鼠的血浆、肠、胃、脾、肾、肝、心和脑等组织中；由于其极性低，北美芹素可以通过血脑屏障[5]。此外，在植物中的研究表明，北美芹素可增强水稻抗稻瘟病以及抗严寒的能力[6]。上述研究表明北美芹素具有多种功能，但它是否可以作为治疗肿瘤的潜在化合物，目前尚无相关报道。

实体肿瘤在不断增殖恶化过程中，其内部由于血管的异常等原因往往呈现氧气极低的一种微环境状态，即低氧微环境。低氧条件下的肿瘤细胞会诱导重要转录因子 HIF-1α 的上调，并通过 HIF-1α 调控多种细胞生物学行为，如细胞增殖、凋亡、代谢、转移、自噬等来适应这种恶性的肿瘤微环境而存活下来[7-8]。另一方面，代谢异常被认为是肿瘤的重要特征之一，实体瘤内部最经典的代谢改变当属瓦博格效应（Warburg Effect），即肿瘤细胞倾向于使用糖酵解的方式将葡萄糖代谢为丙酮酸，进而转化成乳酸并生成 ATP。其中，葡萄糖代谢相关的多数代谢酶均受到 HIF-1α 的转录调控，并在肿瘤中高度活化[9-10]。但是，北美芹素是否通过调控代谢进而影响肿瘤细胞在微环境下的存活，目前并未见相关研究报道。

为了探究北美芹素是否具有抗肿瘤作用，我们首先利用体外培养的肿瘤细胞展开研究，发现北美芹素可以明显抑制多种肝癌细胞的增殖，而且这种抑制现象在低氧条件下更为明显；通过机制探究，我们发现北美芹素可降低 HIF-1α 的蛋白水平并下调多

种葡萄糖代谢酶的表达；进一步小鼠体内实验结果表明，北美芹素可以通过抑制糖代谢途径的激活从而抑制肝癌的发生和发展；最后，我们利用临床肝癌病人来源的肝癌类器官模型发现，在一定浓度范围内，北美芹素可以明显抑制肝癌病人来源的肝癌类器官的生长，但对正常肝组织来源的类器官的生长无明显副作用。这些结果表明，北美芹素在体、体内外均可显著地抑制肝癌的发生发展，提示北美芹素是潜在的靶向肿瘤生长的中草药化合物，这些研究结果为中草药化合物有效预防、治疗肿瘤提供了新的重要证据。

2. 实验材料与方法

2.1 细胞培养和试剂

人肝癌细胞系 Hep3B、PLC 和 HepG2（购自 ATCC 细胞库），使用 DMEM 培养基并加入 10%的血清和 1%的双抗，在 37 ℃，5% CO_2 的细胞培养箱中进行培养。北美芹素处理时，加入相应浓度的北美芹素，并使用 DMSO 作为对照，处理相应的时间。低氧处理时，将需要处理的细胞放置于低氧工作站（Don Whitley Scientific）内处理相应的时间。

蛋白免疫印迹实验检测的抗体 HIF-1α, LDHA, PKM2, GLUT1 和 Actin 均购自武汉三鹰生物技术有限公司；药物处理实验用到的 DMOG, DFX, $CoCl_2$ 和 MG-132 均购自于上海陶素生化科技有限公司。

2.2 药物筛选

29 种天然中草药来源的化合物库购于上海陶素生化科技有限公司（Targetmol, Shanghai）。这些化合物均是从中国各地普通民众极易获得的黄芩、黄芪、丹参、紫花前胡、肉苁蓉等中草药提取而来。用 DMSO 溶解每种化合物并配制成母液。在 24 孔板中的每个孔预先种植 2×10^4 个 Hep3B 细胞，待细胞贴壁后在每个孔中加入工作浓度为 100 uM 的天然化合物，对照孔加入等稀释比例的 DMSO 作为对照。经过 96 小时的处理以后，通过结晶紫染色的方法，对每个孔中的细胞进行染色，染色的强度代表了药物处理后剩余活细胞的数量，相应的可以来评估药物对细胞的杀伤能力。

2.3 结晶紫染色实验

待细胞培养或药物处理之后，弃去培养液，用 PBS 小心洗涤 1-2 次，去除残余培养基；甲醇固定 20min，0.1% 结晶紫染色 15-20min，用 PBS 洗掉多余的染色剂；自然干

燥或 37℃烘干后，利用扫描仪对结晶紫染色的细胞培养板进行扫描；此板可以在室温中长期保存。注：结晶紫是先配成 0.5%的母液（称 0.5 g 结晶紫，溶到 100 ml PBS 中），使用时再用 PBS 稀释。

2.4 MTT 法测定半抑制浓度 IC50

2.4.1：接种细胞

调零组：DMEM

对照组：细胞＋DMEM

实验组：细胞＋DMEM＋北美芹素

用含 10%胎小牛血清的 DMEM 将细胞制成单细胞悬液，以每孔 6000 个/100 ul 接种到 96 孔板中。

2.4.2：加药处理

细胞培养 24 小时贴壁后，通过倍比稀释法加药处理，每个药物浓度 6 个平行。

2.4.3：呈色

培养 48 小时后，对照组、加药组及调零组每孔加噻唑兰（MTT）溶液（5mg/ml）10 ul。继续孵育 4 小时后终止培养，每孔加入 100 ul 三联液，保鲜膜封好后放置 37℃培养箱 4 小时。

2.4.4：比色

使用酶标仪 570nm 波长测定各孔吸光值（OD570），记录结果。细胞相对活力表示为 [OD570（加药组）- OD570（调零组）] / [OD570（对照组）- OD570（调零组）] × 100%。以药物浓度为横坐标，细胞相对活力为纵坐标，通过 Graphpad Prism 软件绘制拟合曲线，计算出 IC50。

2.5 总 RNA 提取和 qRT-PCR 实验

2.5.1 总 RNA 的提取

1）用 PBS 洗 6 cm 皿中的细胞，而后除净皿中的 PBS

2）向每个皿中加入 1 ml 的 trizol 裂解细胞，并收集样品到 RNA 酶 free 的离心管中

3）每个样品管中加入 200 ul 三氯甲烷，上下颠倒混匀 5-6 次并室温放置 2-3 分钟直至分层

4）8,000 x g 4℃离心 15 分钟

5）将离心后的 EP 管轻轻取出，45 度角倾斜，用移液枪将上层的水相取出

6）将上层水相转移到新的 RNA 酶 free 的 EP 管中

7）加入 500 ul 的异丙醇到水相中，并在室温下敷育 10 分钟

8）10,000 x g　4℃离心 15 分钟

9）轻轻移去上清，只留下 RNA 沉淀。洗涤沉淀，加入 1 ml 75%乙醇到 RNA 沉淀中，轻轻的上下颠倒 EP 管，然后 10,000 x g 4℃离心 15 分钟。弃去洗涤液

10）用真空泵吸干或者静置风干 RNA 沉淀 10 分钟。加入 0.1% DEPC 水溶解 RNA 并利用 NanoDrop 测定 RNA 浓度

2.5.2　第一链 cDNA 的合成

1） 在 200 ul 的 PCR 管中 set up 下述反应体系：

成分	体积/每反应
5x iScript reaction mix	4 µl
iScript reverse transcriptase	1 µl
Nuclease-free water	(15-x) µl
RNA (1 µg total RNA)	x µl
Total volume	20 µl

2） PCR 反应合成第一链 cDNA

25℃ 5 分钟

42℃ 30 分钟

85℃ 5 分钟

4℃维持或者直接转入-20℃冻存起来

2.5.3　PCR 或 qRT-PCR 反应

1)所有的引物母液用 DNA/RNA 酶 free 的水稀释至 100 uM，而后 Forward 引物、Reverse 引物各取 10 ul，加 DNA/RNA 酶 free 的 80 ul 水至 100 ul 配制成 10 uM 的（Fwd + Rev）引物工作混合液

2)用 DNA/RNA 酶 free 的水 10 倍稀释 cDNA（10 ul cDNA + 90 ul DNA/RNA 酶 free water）

3）轻轻混匀并短暂离心 SYBR Green

4）在冰上准备 PCR 反应混合液并轻轻混匀，短暂离心

SYBR Green (2 X)	10 µl
Primer (Fwd + Rev) 10 uM	0.4 ul

cDNA (1：10)	2.0 ul
Water, nuclease-free	7.6 μl
Total volume	20 μl

5）利用下述步骤准备 qRT-PCR 反应体系

步骤	反应温度（℃）	反应时间	循环次数
预变性	94	30 s	1
变性	94	30 s	25-40 循环
退火	Tm-5 (55~65)	30 s	
延伸	72	30 s	
最终延伸	72	7 min	1

2.5.4 本文中所用基因引物序列如下：

基因名 （Gene Name）	引物序列 （Primer Sequence）
Hs-18S-Fwd	CGGCGACGACCCATTCGAAC
Hs-18S-Rev	GAATCGAACCCTGATTCCCCGTC
Hs-LDHA-Fwd	GGCTACAACAGGATTCTA
Hs-LDHA-Rev	TTACAAACCATTCTTATTTCTAAC
Hs-PKM2-Fwd	ATAACGCCTACATGGAAAAGTGT
Hs-PKM2-Rev	TAAGCCCATCATCCACGTAGA
Hs-PDK1-Fwd	ACCAGGACAGCCAATACAAG
Hs-PDK1-Rev	CCTCGGTCACTCATCTTCAC
Hs-Glut1-Fwd	CGGGCCAAGAGTGTGCTAAA
Hs-Glut1-Rev	TGACGATACCGGAGCCAATG
Hs-Glut2-Fwd	GCTGCTCAACTAATCACCATGC
Hs-Glut2-Rev	TGGTCCCAATTTTGAAAACCCC
Hs-Glut3-Fwd	GCTGGGCATCGTTGTTGGA
Hs-Glut3-Rev	GCACTTTGTAGGATAGCAGGAAG
Hs-Glut4-Fwd	ATCCTTGGACGATTCCTCATTGG
Hs-Glut4-Rev	CAGGTGAGTGGGAGCAATCT
Hs-PGK1-Fwd	GACCTAATGTCCAAAGCTGAGAA
Hs-PGK1-Rev	CAGCAGGTATGCCAGAAGCC
Hs-TPI1-Fwd	AAAGCTGGTGCCGTTGAGAA
Hs-TPI1-Rev	GGTTGTGGTAAACCTCTGCTC
Hs-PFKL-Fwd	GTACCTGGCGCTGGTATCTG
Hs-PFKL-Rev	CCTCTCACACATGAAGTTCTCC
Hs-SCD1-Fwd	AGAATGGAGGAGATAAGT
Hs-SCD1-Rev	TAGCAGAGACATAAGGAT
Hs-HK2-Fwd	CCAGTTCATTCACATCATCAG

Hs-HK2-Rev	CTTACACGAGGTCACATAGC
Hs-ENO1-Fwd	GCCGTGAACGAGAAGTCCTG
Hs-ENO1-Rev	ACGCCTGAAGAGACTCGGT
Hs-G6PD-Fwd	ACCGCATCGACCACTACCT
Hs-G6PD-Rev	TGGGGCCGAAGATCCTGTT
Hs-HIF-1α-Fwd	GAACGTCGAAAAGAAAAGTCTCG
Hs-HIF-1α-Rev	CCTTATCAAGATGCGAACTCACA

2.6 蛋白提取及聚丙烯酰胺凝胶电泳操作（Western blotting）

1）在 10 cm 培养皿中培养细胞

2）用 10 ml 预冷的 1 x PBS 清洗细胞两次，将 8 ml 冷的 1 x PBS 倒入培养皿中，用细胞刮刀收集细胞至 15 ml 离心管中，然后 3000 rpm 转速 4 度离心 5 分钟，弃上清

3）加入适当量的蛋白裂解液 RIPA Buffer（50 mM Tris–HCl, pH 8.0, 150 mM NaCl, 5 mM EDTA, 0.1% SDS, 1% NP-40, cocktail）裂解细胞，并转移样品到预冷的 EP 管中

4）将样品放置冰上 45~60 分钟，中间涡漩混匀 2-3 次

5）将蛋白裂解液在 14,000 rpm 转速下 4℃离心 10 分钟

6）转移蛋白上清至新的预冷的 EP 管中

7）蛋白定量：裂解好的蛋白样品在 4℃条件下用 12,000 rpm 离心 10 min，将蛋白样品上清转移到新预冷的 1.5 ml 离心管中。采用 Bradford 标准曲线法定量蛋白浓度

8）浓度定好后加入 5 x Loading buffer，100℃煮 5 分钟

9）上样：上同样量的蛋白样品并带上蛋白 marker

10）首先在 80 v 电压下电泳，待到样品完全跑出浓缩胶以后将电压调至 120 v 继续分离约 1 h

11）利用湿转法转膜约 1.5 h-2 h

12）待转膜结束以后，用 1 x washing buffer 配置的 5% 脱脂牛奶（NFDM）封闭 NC 膜或 PVDF 膜约 1 小时

13）封闭完成以后一抗敷育约 1.5 小时，用 1 x washing buffer 洗 NC 膜或 PVDF 膜 3 x 10 分钟

14）相应种属来源的二抗敷育约 1.5 小时，用 1 x washing buffer 洗 NC 膜或 PVDF 膜 3 x 10 分钟

15）将膜取出放在塑料膜或保鲜膜（saran wrap）上，加入 ECL 显影液。混合等体积的两种 ECL 试剂并均匀平铺在 NC 膜或 PVDF 膜上，将膜放在化学发光显影仪器中进行

显影

2.7 小鼠移植瘤治疗模型

利用 4 周左右的雄性 BALB/c 裸鼠，将 500 万 Hep3B 细胞注射在小鼠的腹部皮下组织。在第 10 天，用不同浓度（0.08mg/kg，0.3mg/kg，1.5mg/kg）的北美芹素进行小鼠灌胃处理，对照组小鼠给予相应稀释浓度的 DMSO。在给药后，每隔三天使用游标卡尺对小鼠肿瘤大小进行测量体积，计算公式：肿瘤体积= 长 （mm）x 宽（mm）x 高（mm）x 0.52。在第 26 天，对小鼠进行称重并处死，并取出其中的肿瘤，进行蛋白的提取及蛋白水平检测。

2.8 小鼠移植瘤预防模型

利用 4 周左右的 BALB/c 裸鼠，预先使用 0.08mg/kg 北美芹素进行灌胃处理，对照组小鼠给予相应稀释浓度的 DMSO。灌胃处理 10 天后，将 500 万 Hep3B 细胞注射在小鼠的腹部皮下组织。之后，每隔 2-3 天使用游标卡尺对小鼠肿瘤大小进行测量，计算公式式：肿瘤体积= 长 （mm）x 宽（mm）x 高（mm）x 0.52。在第 30 天，对小鼠进行处死，并取出其中的肿瘤，检测肿瘤大小。

2.9 类器官的药物处理及活力检测

用 0.25% Trypsin-EDTA 分别将临床肝癌病人来源的肝癌类器官和正常肝脏类器官进行消化处理，消化成单细胞后计数，用 2% BME/培养基重悬，按照 5000 个细胞/孔，加入到预先用 30 ul / 孔 BME 包被好的 96 孔板中，培养 3 天后，更换成加药处理的培养基，处理 6 天，每隔 3 天换一次液。

用药物处理 6 天后，进行细胞活力检测，加入与培养基等比例的 CellTiter-Glo 3D 试剂（promega），震荡 5 分钟，室温静置 20 分钟以稳定信号，之后使用 SynergyH1 多功能酶标仪，测量发光值。结果与对照组进行对比（DMSO 组），并采用 Prism（GraphPad）软件和非线性回归方程进行曲线拟合。类器官形态变化的照片是在与上述细胞活力检测相同的处理条件下，用药物处理 6 天后，利用普通光学显微镜的白光视野，在 10 倍物镜条件下拍摄 24 孔板中的类器官所得。

qRT-PCR 检测 organoid 中基因变化：将消化处理过的 organoid 用 BME 重悬后 seed 到 6 孔板中，37 度培养箱培养 6 天后，分别加入 DMSO，50 uM pteryxin，100 uM pteryxin，放入 1% O_2 的低氧工作站中处理 24 小时。在第 8 天时，使用（Magen R4111-02)

Hipure total RNA mini kit 进行 RNA 抽提。逆转录及后面的操作与上述“2.5 总 RNA 提取和 qRT-PCR 实验”操作相同。

3. 实验结果

3.1 北美芹素抑制肝癌细胞的增殖，低氧条件下作用更为显著

为了筛选得到潜在的具有抗癌作用的中草药化合物，我们从公司购买获得包含 29 种中草药的小型化合物库，检测工作浓度为 100 uM 时这些化合物对 Hep3B 肝癌细胞的增殖抑制作用。实验结果表明，次黄芩素、隐丹参酮、丹参酮 I、丹参酮 IIA、北美芹素和盐酸巴马汀（黄藤素）处理细胞 96 小时后，肝癌细胞几乎不增殖并且死亡（**图 1A**）。其中部分化合物抑制肿瘤的效果已经有一些相关报道[11-15]，但北美芹素对肿瘤的抑制作用并未见相关报道。因此，接下来我们集中研究了北美芹素对肝癌的抑制作用并探究了其潜在的分子机制。

为了进一步探究北美芹素的抑癌作用是否具有普适性，我们在 Hep3B，PLC 和 HepG2 三种肝癌细胞株中，分别用 10 uM、20 uM、50 uM、100 uM 和 200 uM 北美芹素处理细胞 96 小时，发现北美芹素均可抑制这些肝癌细胞的增殖，并且 50 uM 北美芹素可以部分抑制肝癌细胞的增殖，而 100 uM 北美芹素处理细胞时，细胞基本完全死亡（**图 1B**）。接下来我们通过 MTT 实验，在 Hep3B 细胞系中进行了半抑制浓度的检测，确定北美芹素对 Hep3B 细胞的半抑制浓度为 37.1 uM（**图 1C**）。因为低氧是肝癌这种实体瘤的重要微环境，我们将 Hep3B 细胞放在常氧、低氧条件下分别加对照溶剂 DMSO 或北美芹素处理 96 小时后，发现北美芹素虽然在常氧、低氧条件下均可抑制细胞的增殖，但在低氧条件下对细胞增殖的抑制作用更为明显（**图 1D**）。以上实验结果表明，北美芹素可以抑制肝癌细胞的增殖，并在低氧下抑制作用更为显著。

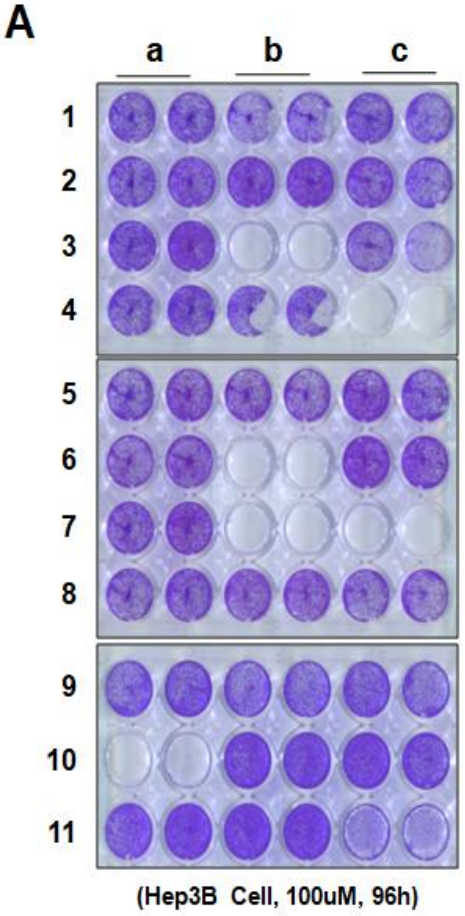

Rank	Name	Chinese Name	Antitumor Effect	Remark (about antitumor effect)
1b	Baicalein	黄芩素	+	
1c	Malic acid	苹果酸	-	
2a	Scutellarein	野黄芩素	-	
2b	Scutellarin	野黄芩苷	-	
2c	Baicalin	黄芩苷	-	
3a	Wogonoside	次黄芩苷	-	
3b	Wogonin	次黄芩素	+++	Known
3c	Cycloastragenol	环黄芪醇	+	
4a	AstragalosideIV	黄芪甲苷	-	
4b	AstragalosideIII	黄芪皂苷III	-	
5b	Tanshinone IIA-sulfonic sodium	丹参酮IIA磺酸钠	-	
5c	Sodium Danshensu	丹参素钠	-	
6a	Calycosin	毛蕊异黄酮	-	
6b	Cryptotanshinone	隐丹参酮	+++	Known
6c	Salvianolic acid B	丹酚酸B	-	
7a	Salvianolic Acid C	丹酚酸C	-	
7b	Tanshinone I	丹参酮I	+++	Known
7c	Tanshinone IIA	丹参酮IIA	+++	Known
8a	Dihydrotanshinone I	二氢丹参酮I	-	
8b	Paeonol	芍药醇	-	
8c	Protocatechuic acid	原儿茶酸	-	
9b	Protocatechualdehyde	原儿茶醛	-	
9c	D-Mannitol	甘露醇	-	
10a	(+)-Pteryxin	北美芹素	+++	Unknown
10b	Allitol	蒜糖醇	-	
10c	4-Hydroxybenzyl alcohol	对羟基苯甲醇	-	
11a	Tubuloside A	管花苷A	-	
11b	Cordycepin	虫草素	-	
11c	Palmatine chloride	盐酸巴马汀	++	Known

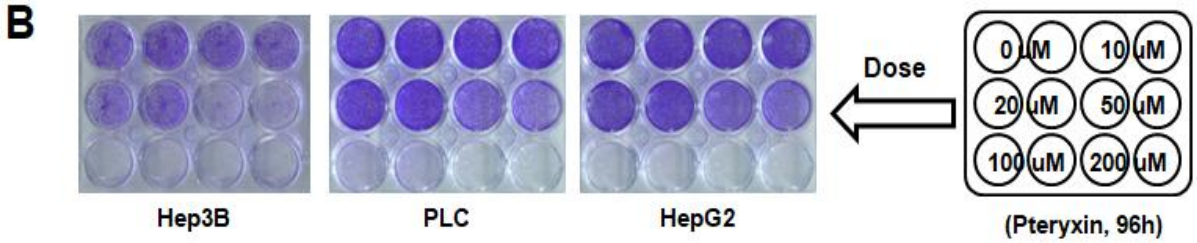

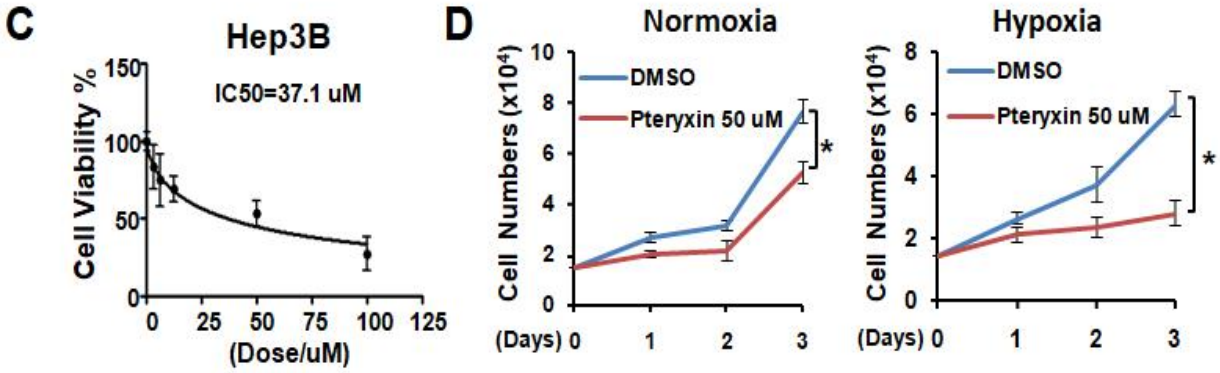

图 1：北美芹素抑制肝癌细胞的增殖，低氧条件下作用更为显著

（**A**）利用 29 种中草药来源的天然化合物（100μM）处理 Hep3B 肝癌细胞 96 小时后进行结晶紫染

色，观察这些天然化合物对细胞增殖的抑制作用（左）；右侧表格总结了天然化合物抑制细胞增殖的筛选结果（右）。（**B**）Hep3B，PLC 和 HepG2 细胞分别用 0 uM，20 uM，50 uM，100 uM 和 200 uM 的北美芹素处理 96 小时后进行结晶紫染色，观察北美芹素对细胞增殖的抑制作用。（**C**）MTT 分析检测北美芹素处理 Hep3B 细胞 48 小时后的细胞活力，并计算其半抑制浓度（IC50）。（**D**）在常氧、低氧条件下利用 50 uM Pteryxin 处理 Hep3B 细胞，利用台盼蓝染色计数绘制细胞增殖曲线。

3.2 北美芹素显著抑制低氧诱导的葡萄糖代谢酶表达

由于北美芹素在低氧条件下的抑癌效果更为明显，因此我们进一步探究了其和低氧的关系。将 Hep3B 细胞在常氧、低氧及低氧下加入北美芹素处理 24 小时后，我们收集 RNA 并进行 RNA-seq 测序分析。结果发现，低氧处理组相对于常氧处理组表达上调大于 1.5 倍的基因有 604 个，低氧处理组相较于低氧加北美芹素处理组表达上调大于 1.5 倍的基因有 3071 个；在这两种比较条件下，共同表达差异都超过 1.5 倍的基因有 392 个（**图 2A**）。对这 392 个基因进行分析并归类后（GO 分析）(DAVID: https://david.ncifcrf.gov/)，发现糖代谢相关基因（包括糖酵解和糖异生相关基因）及低氧相关基因的变化十分明显（**图 2B**）。

接下来，我们分别在常氧、低氧条件下利用 100uM 的北美芹素处理 Hep3B 细胞 24 小时，检测糖代谢相关代谢酶的 mRNA 表达水平。结果表明，北美芹素可以显著抑制低氧条件下表达上调的糖代谢酶如乳酸脱氢酶 A（LDHA）、丙酮酸激酶 M2（PKM2）、丙酮酸脱氢酶激酶同功酶 1（PDK1）、葡萄糖转运蛋白 1（GLUT1）、磷酸甘油酸激酶（PGK1）等的表达（**图 2C**）。同样条件下，利用北美芹素处理 Hep3B 细胞 48 小时后，我们提取蛋白进行 Western Blotting 分析，发现北美芹素可以明显抑制低氧诱导的糖代谢相关代谢酶的蛋白水平（**图 2D**）。综上所述，北美芹素能够显著抑制肝癌细胞中低氧诱导的葡萄糖代谢酶的 mRNA 及蛋白水平。

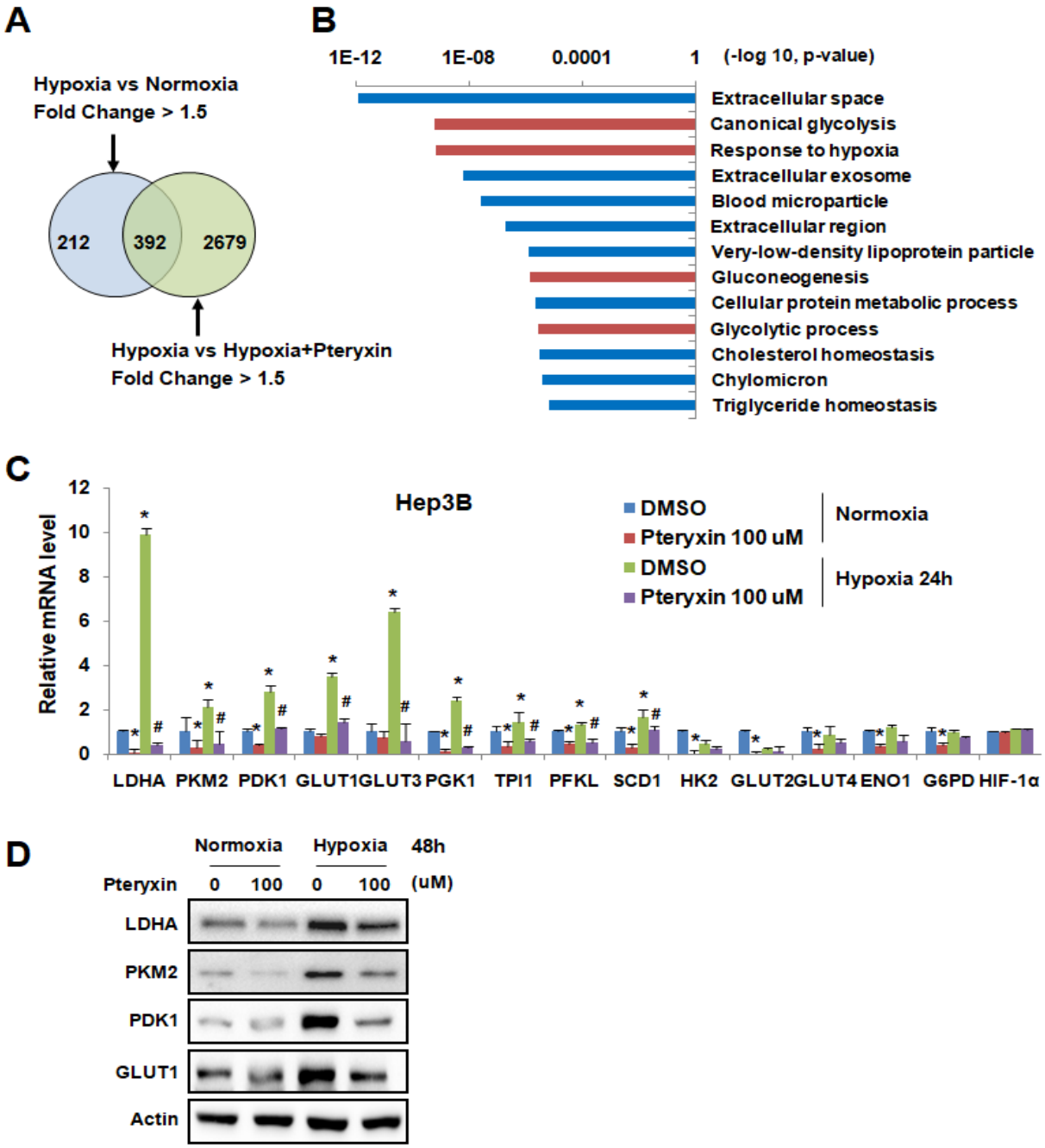

图 2：北美芹素显著抑制低氧诱导的葡萄糖代谢酶表达

（**A**）通过转录组学分析发现，低氧条件下相较于常氧条件表达升高大于 1.5 倍的基因有 604 个；低氧条件下相较于低氧加北美芹素处理组表达升高大于 1.5 倍的基因有 3071 个；然后利用维恩图分析发现在这两种比较条件下，共同表达差异都超过 1.5 倍的基因有 392 个。（**B**）对这 392 个基因进行基因聚类分析（GO 分析）检测其所富集的通路。（**C**，**D**）利用 qRT-PCR（**C**）和 Western blotting（**D**）分析在常氧或低氧条件下，Hep3B 细胞分别用 DMSO 和 100 uM Pteryxin 处理 24 小时或 48 小时后葡萄糖代谢酶的 mRNA 和蛋白水平变化。*指与常氧 DMSO 处理组相比 $P < 0.05$，#指与低氧

DMSO 处理组相比 $P < 0.05$。数据分析方法为 T 检验。

3.3 北美芹素抑制 HIF-1α 的蛋白表达

图 2 的实验结果表明，北美芹素可在转录水平调控葡萄糖代谢酶的表达，而低氧诱导因子 HIF-1α 是低氧诱导表达的重要转录因子，已知 HIF-1α 可在转录水平激活多种葡萄糖代谢酶的表达，但我们并不清楚北美芹素是否可以通过影响 HIF-1α 的表达从而调控糖代谢过程。基于此猜想，我们将 Hep3B 细胞分别放在常氧和低氧条件下，并加入 50uM 的北美芹素处理 6 小时，Western Blot 检测结果发现，低氧条件下 HIF-1α 蛋白的累积在加入北美芹素处理后明显受到抑制（**图 3A**）。我们进一步分别使用 50uM 和 100uM 北美芹素，并在低氧模拟剂 DMOG、DFX、$CoCl_2$ 或蛋白酶体降解途径的抑制剂 MG-132 存在的条件下，处理 Hep3B 细胞，结果发现北美芹素的加入可以剂量依赖性的抑制 HIF-1α 蛋白的表达，并且 DMOG、DFX、$CoCl_2$ 或蛋白酶体抑制剂 MG-132 并不能抑制北美芹素对 HIF-1α 蛋白的这种下调作用（**图 3B**）。而图 2C 的结果表明北美芹素不影响 HIF-1α mRNA 的表达，图 3B 的结果表明北美芹素不影响 HIF-1α 的蛋白降解，因此我们推测，北美芹素可能通过蛋白翻译途径影响 HIF-1α 的蛋白表达从而影响其所介导的功能，这些还需要进一步的实验证明。

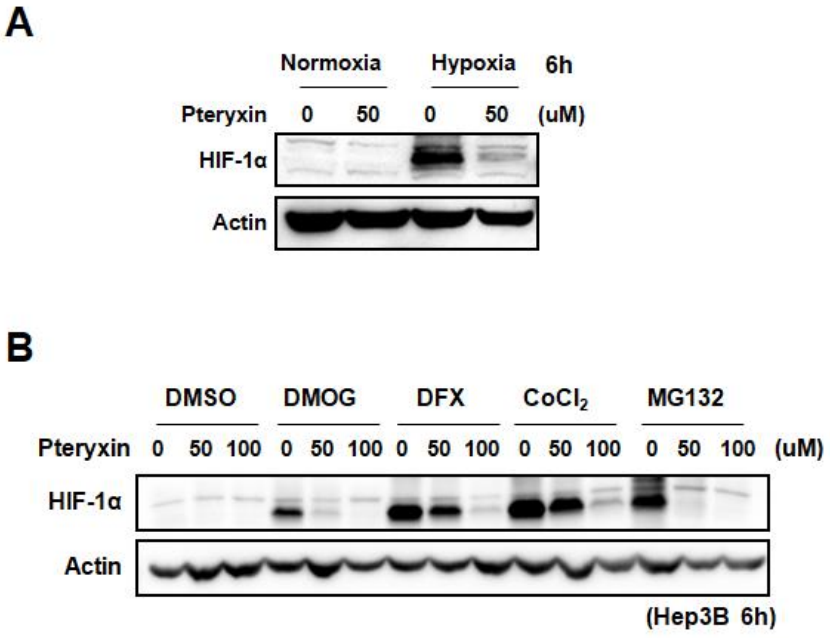

图 3：北美芹素抑制 HIF-1α 的蛋白表达

（**A**）在常氧或低氧条件下，利用 DMSO 或 50 uM 北美芹素处理 Hep3B 细胞 6 小时，提取细胞裂解液，进行免疫印迹 Western blotting 分析，检测 HIF-1α 的蛋白水平。Actin 为内参蛋白。（**B**）将 DMSO，低氧模拟剂（$CoCl_2$、DFX、DMOG）或蛋白酶体抑制剂（MG-132）与 0，50，100 uM 北美芹素进行联合用药处理 Hep3B 细胞，处理 6 小时后提取全细胞裂解液进行 Western blotting 分析，检测 HIF-1α 的蛋白水平。Actin 为内参蛋白。

3.4 北美芹素抑制小鼠模型中肝癌的发生发展

上述体外实验证明，北美芹素可以显著抑制低氧条件下肝癌细胞的增殖，并且抑制 HIF-1α 的蛋白水平以及葡萄糖代谢酶的表达。那么，在小鼠肿瘤模型中是否存在同样的现象呢？我们通过皮下注射肝癌 HepB 细胞构建小鼠移植瘤模型，在皮下肿瘤体积达到约 100 mm^3时，我们将小鼠随机分组，分别进行 DMSO 以及 0.08 mg/kg、0.3 mg/kg、1.5 mg/kg 北美芹素的灌胃给药处理，观察北美芹素对小鼠体内肿瘤生长的抑制情况。经过约一个月时间的跟踪和肿瘤体积测量后，我们发现相较于对照组，饲喂北美芹素的小鼠的肿瘤体积明显下降，并且高浓度的北美芹素处理时，效果更为明显，呈现剂量依赖性效果（**图 4A**）。图 4B 是实验结束时取出的小鼠肿瘤的照片显示结果，可以看到饲喂北美芹素后小鼠肿瘤大小明显减小，而且在较高浓度时，有些小鼠肿瘤已经消退（**图 4B**）。但是实验结束时对这些小鼠进行体重称量分析，我们并未发现这几组小鼠之间体重上有明显差异，提示北美芹素对小鼠带来的副作用较小，这些结果表明它可能是一个潜在的有效抗癌药物（**图 4C**）。最后，我们提取这些小鼠肿瘤组织的蛋白裂解液，通过 Western Blotting 检测发现，与体外细胞水平的结果一致，加入北美芹素确实可以抑制 HIF-1α、PKM2、PDK1 和 LDHA 的蛋白表达（**图 4D**）。综上，小鼠移植瘤实验表明北美芹素可以明显抑制体内肝癌的发生发展，并且可能是通过抑制 HIF-1α 以及葡萄糖代谢酶的表达来实现的。

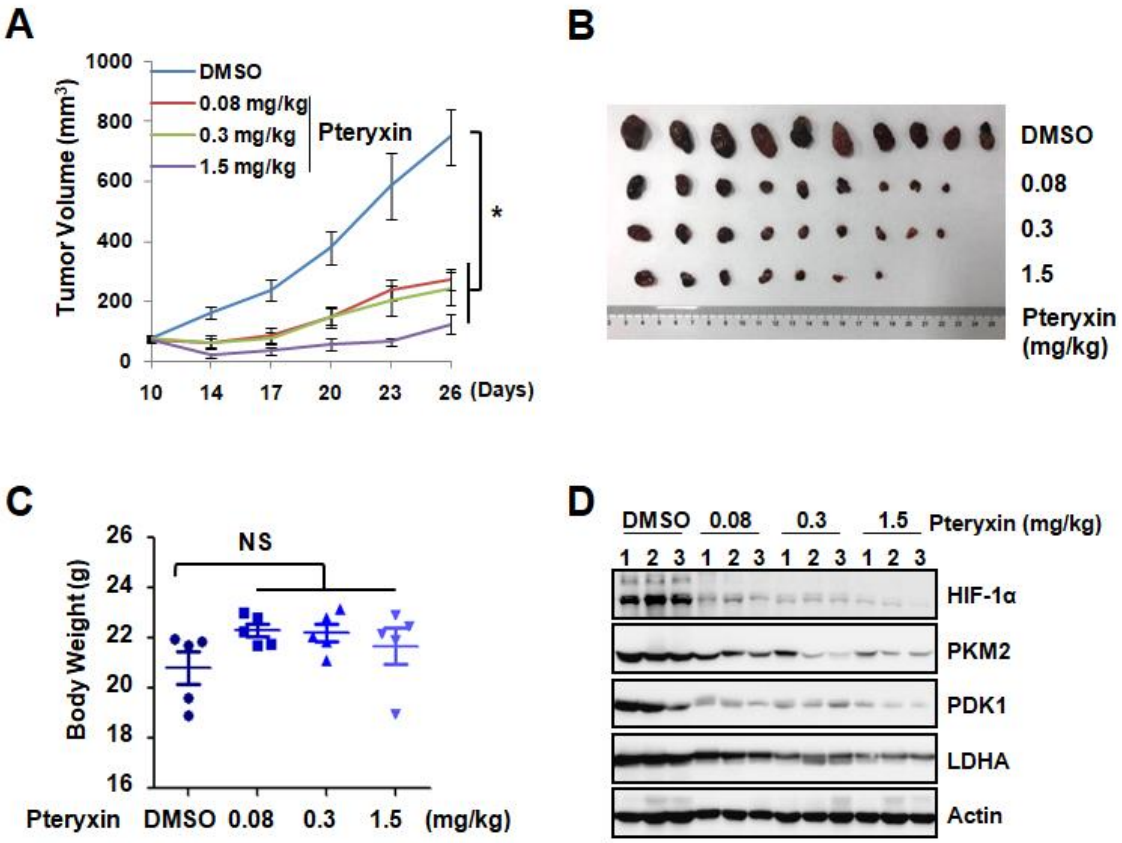

图 4: 北美芹素抑制小鼠模型中肝癌的发生发展

将 Hep3B 细胞皮下注射到裸鼠体内，在肿瘤体积达到约 100 mm^3 时，开始每两天一次给小鼠进行灌胃 DMSO，0.08mg / kg，0.3mg / kg 或 1.5mg / kg 的北美芹素（每组 n = 5 只）。（**A**）从接种后第 10 天开始测量小鼠皮下移植瘤大小，数据表示为平均值±SEM。*指所示组之间 $P < 0.05$。数据分析方法为 T 检验。（**B**，**C**）在实验结束时，提取肿瘤并拍照展示小鼠肿瘤大小（B），同时记录并分析小鼠体重（C）。（**D**）提取小鼠肿瘤组织的蛋白裂解液，进行 Western blotting 分析，检测 HIF-1α 和葡萄糖代谢酶的蛋白水平。Actin 为内参蛋白。

3.5 北美芹素有效预防小鼠模型中肝癌的发生

那么，北美芹素是否可以预防肝癌的发生呢？在另外一种小鼠移植瘤模型中，我们预先使用 0.08 mg/kg 的低浓度北美芹素对小鼠进行灌胃给药预处理，10 天之后再对小鼠进行肿瘤细胞的皮下注射，来观察北美芹素是否可以预防小鼠肝癌的发生。在跟踪观察小鼠的前期，我们可以明显看到北美芹素处理组的小鼠肿瘤出现的时间点发生后移，且肿瘤体积与对照组相比也明显减小；在北美芹素处理 30 天后，与对照组相比，

肿瘤的体积显著减小（**图 5A**）。B 图显示的是实验结束时取出的小鼠肿瘤的照片结果（**图 5B**）。因此，这个实验结果表明北美芹素可以预防肝癌的发生，提示可以通过日常补充北美芹素来预防肝癌的可能性。

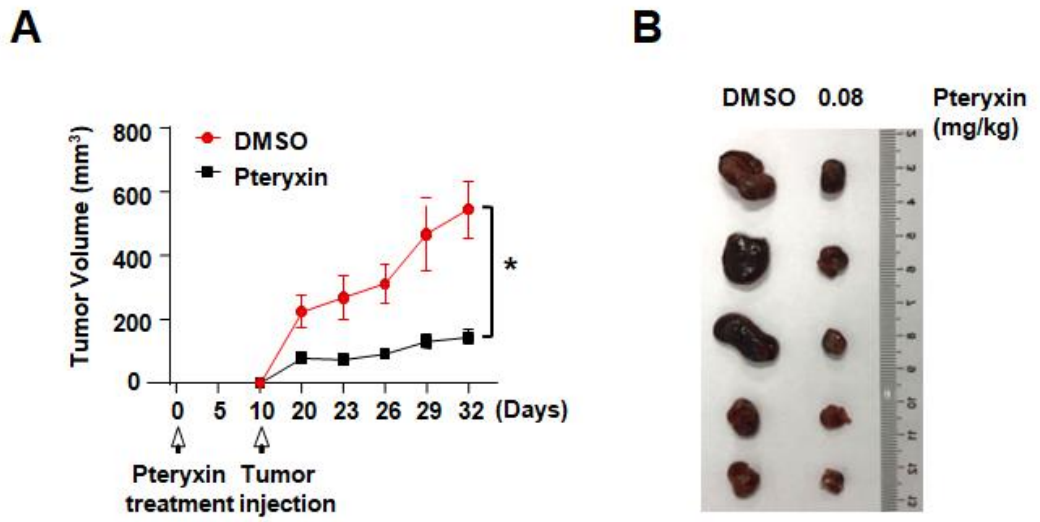

图 5：北美芹素有效预防小鼠模型中肝癌的发生

（**A**）从第 0 天开始，每两天一次给小鼠灌胃 DMSO 或 0.08 mg / kg 北美芹素，建立肿瘤预防模型。在第 10 天将 Hep3B 细胞注射到裸鼠皮下（每组 n = 5 只），并持续灌胃给药，追踪测量肿瘤大小，数据表示为平均值±SEM。 *指所示组之间 P < 0.05。数据分析方法为 T 检验。（**B**）在实验结束时，提取肿瘤并拍照展示小鼠肿瘤大小。

3.6 北美芹素抑制临床肝癌病人组织来源的肝癌类器官的生长和葡萄糖代谢

类器官研究体系是在培养皿中进行细胞培养的基础上发展起来的一种三维微器官培养模型，它与来源组织和器官高度相似，比体外培养的细胞更加接近于临床病人的实际情况，能够帮助我们更好的检验药物的功效 [16, 17]。因此，接下来，我们利用来源于临床肝癌病人组织的肝癌类器官模型和正常人肝组织的类器官模型进行北美芹素药效的评估。我们发现在临床肝癌病人组织的肝癌类器官模型中，北美芹素对细胞增殖的半抑制浓度为 49.33 uM，这个数值远低于正常肝组织诱导的类器官中的 IC50（103 uM）（**图 6A**），这说明北美芹素在较低浓度时即可抑制肝癌类器官的增殖，即肝癌组织对北美芹素更为敏感，同时其对正常组织细胞的抑制作用相对较小，可以保护正常细胞免受毒害。而直观的显微镜下的观察也发现，加入北美芹素 50 uM 或 100 uM，可以

显著抑制临床肝癌病人组织来源类器官的生长和增殖，而对正常肝组织来源的类器官则没有明显影响（**图 6B**）。进一步提取 RNA 检测常氧、低氧条件处理的类器官中葡萄糖代谢酶的表达，结果发现，与之前在体外培养细胞中的结果一致，加入北美芹素后，可以抑制低氧诱导的葡萄糖代谢酶的 mRNA 水平（**图 6C**）。上述实验表明，北美芹素确实可以抑制临床肝癌病人组织来源的肝癌类器官的生长及其葡萄糖代谢酶的表达，暗示其具有较好的临床适用性。

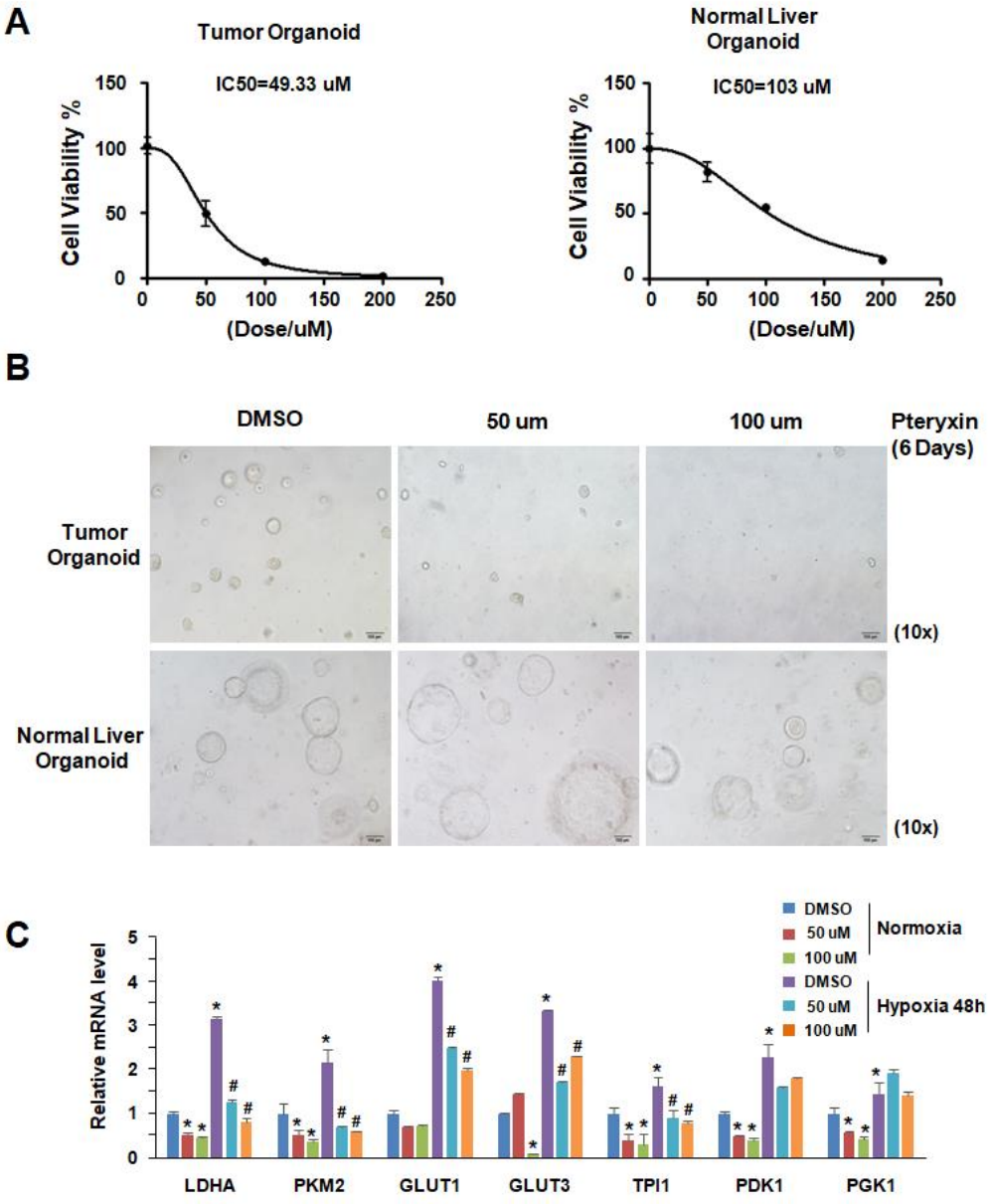

图 6：北美芹素抑制临床肝癌病人组织来源的肝癌类器官的生长和葡萄糖代谢

（**A**）分别在临床肝癌病人来源的肝癌类器官（左）及正常肝脏类器官（右）模型中，加入 DMSO，

50 uM，100 uM 和 200 uM 北美芹素，处理 6 天后，使用 CellTiter-Glo 3D 试剂，检测类器官的活力，并计算其半抑制浓度（IC50）。（**B**）明场图片展示 50 uM，100 uM 北美芹素处理 6 天后对在临床肝癌病人来源的肝癌类器官（上）及正常肝脏类器官（下）克隆形成的影响。标尺：100 um。（**C**）利用 qRT-PCR 分析常氧和低氧条件下，临床肝癌病人来源的肝癌类器官模型中分别加入 DMSO，50 uM 和 100 uM 北美芹素处理 48 小时后葡萄糖代谢酶 mRNA 水平的表达。

4. 结论与展望

通过对一系列中草药来源化合物的筛选，本课题发现北美芹素可以抑制肝癌细胞的增殖，并且发现低氧条件下其抑制效果更为明显。大数据分析和后续实验证明，北美芹素可以抑制低氧条件下重要转录因子 HIF-1α 及葡萄糖代谢通路相关酶的表达从而抑制肿瘤生长。在小鼠移植瘤的治疗和预防模型中，我们均发现北美芹素可明显抑制肝癌的发生和发展，并且无明显毒副作用。进一步在临床肝癌病人或正常肝组织来源的类器官模型中，也能观察到北美芹素显著抑制临床肝癌病人组织来源类器官的生长和增殖，而对正常肝组织来源的类器官则没有明显影响。基于以上实验结果，北美芹素可以在体内、体外的肝癌细胞水平、小鼠移植瘤模型以及临床肝癌病人的类器官模型中抑制肝癌的发生发展，这些数据表明北美芹素是一种潜在的治疗肿瘤的中草药化合物，本研究对中草药化合物预防和治疗肿瘤的开发利用具有重要的指导意义。

当前人们对肿瘤并没有非常彻底且完美的治疗方法，因此抗肿瘤药物的研发仍然是重中之重。中药在历经数千年的使用后，已被证明其针对肿瘤治疗的有效性，但多数中药的有效成分及潜在抗癌机制仍远未明了。因此，从中药中寻找合适的化合物并探究其潜在的抗癌机制，一直是抗肿瘤药物研究领域的热点，而本研究中潜在的抗肿瘤化合物北美芹素被筛选出来，则是十分有意义且令人兴奋的结果。之前已有报道探究了北美芹素的药代动力学，并发现其可以抑制肥胖和抵抗炎症发生，但是其对肿瘤的影响仍不为人知。本研究中，我们利用不同的体内、体外模型均证明了北美芹素具有很好的肿瘤预防和治疗效果且对正常组织的毒副作用较小，潜在的机制研究表明北美芹素可通过抑制 HIF-1α 和葡萄糖代谢来抑制肝癌的发生发展。由于北美芹素易被摄取和代谢，相对来说，对人体的毒副作用较小，而之前的报道也发现它对生物个体是有益的，因此，北美芹素作为一个潜在的临床预防和治疗肿瘤的药物，其前景非常值得期待及进一步的探索。

综上所述，系统探究北美芹素抗癌的具体分子机制，并阐明它是否在其他类型肿瘤中具有普适性，均具有重要的临床意义。此外，是否可以将北美芹素进一步优化、开发并与其他肿瘤治疗方法如免疫治疗等联用来防治肿瘤，也值得我们进一步探索。

5. 致谢

本论文是在华南理工大学医学院孙林冲老师的悉心指导和精心组织下完成的。在这两年多的时间里，从我理论、技术的学习到实验设计、论文撰写等都倾注了孙林冲老师无数的心血和汗水。同时，感谢孙老师课题组的研究生陈锐、陆慧、林志远、张洋等在实验操作及数据分析等方面的帮助，我从他们身上学到了很多。感谢北京诺禾致源公司提供的 RNA 测序结果。尽管本课题还有很多值得改进并进一步深入探讨的地方，但是这段科研经历对我来讲是弥足珍贵的，从中我体会到了科研的乐趣，同时也深刻体会到了坚定的毅力和坚持下去的决心在科研中的重要性，这些研究在锻炼我能力的同时也磨练了我原本心急浮躁的性格，对我的成长意义非凡。值此论文完成之际，谨向帮助、指导我的各位老师、同学、朋友表示衷心的感谢。

6. 参考文献

1. Matsuda, H., Murakami, T., Kageura, T., Ninomiya, K., Toguchida, I., Nishida, N., and Yoshikawa, M. (1998). Hepatoprotective and nitric oxide production inhibitory activities of coumarin and polyacetylene constituents from the roots of Angelica furcijuga. Bioorganic & medicinal chemistry letters *8*, 2191-2196.
2. Nugara, R.N., Inafuku, M., Takara, K., Iwasaki, H., and Oku, H. (2014). Pteryxin: a coumarin in Peucedanum japonicum Thunb leaves exerts antiobesity activity through modulation of adipogenic gene network. Nutrition (Burbank, Los Angeles County, Calif) *30*, 1177-1184.
3. Yoshikawa, M., Nishida, N., Ninomiya, K., Ohgushi, T., Kubo, M., Morikawa, T., and Matsuda, H. (2006). Inhibitory effects of coumarin and acetylene constituents from the roots of Angelica furcijuga on D-galactosamine/lipopolysaccharide-induced liver injury in mice and on nitric oxide production in lipopolysaccharide-activated mouse peritoneal macrophages. Bioorganic & medicinal chemistry *14*, 456-463.

4. Nugara, R.N., Inafuku, M., Takara, K., Iwasaki, H., and Oku, H. (2014). Pteryxin: a coumarin in Peucedanum japonicum Thunb leaves exerts antiobesity activity through modulation of adipogenic gene network. Nutrition (Burbank, Los Angeles County, Calif) *30*, 1177-1184.
5. Wang, J., Ma, Y., Li, W., Hu, F., Chen, T., Shen, X., and Feng, S. (2012). Study on pharmacokinetics and tissue distribution of pteryxin in mice by ultra-pressure liquid chromatography with tandem mass spectrometry. Biomedical chromatography : BMC 26, 802-807.
6. 柏连阳，陈桂华，刘二明，et al. 北美芹素在诱导水稻抗稻瘟病和抗寒性中的应用: CN.CN101766172 B.
7. Semenza, G.L. (2003). Targeting HIF-1 for cancer therapy. Nature reviews Cancer *3*, 721-732.
8. Majmundar, A.J., Wong, W.J., and Simon, M.C. (2010). Hypoxia-inducible factors and the response to hypoxic stress. Molecular cell *40*, 294-309.
9. Vander Heiden, M.G., Cantley, L.C., and Thompson, C.B. (2009). Understanding the Warburg effect: the metabolic requirements of cell proliferation. Science (New York, NY) *324*, 1029-1033.
10. Koppenol, W.H., Bounds, P.L., and Dang, C.V. (2011). Otto Warburg's contributions to current concepts of cancer metabolism. Nature reviews Cancer *11*, 325-337.
11. Li-Weber, M. (2009). New therapeutic aspects of flavones: the anticancer properties of Scutellaria and its main active constituents Wogonin, Baicalein and Baicalin. Cancer treatment reviews *35*, 57-68.
12. Shin, D.S., Kim, H.N., Shin, K.D., Yoon, Y.J., Kim, S.J., Han, D.C., and Kwon, B.M. (2009). Cryptotanshinone inhibits constitutive signal transducer and activator of transcription 3 function through blocking the dimerization in DU145 prostate cancer cells. Cancer research *69*, 193-202.
13. Lee, C.Y., Sher, H.F., Chen, H.W., Liu, C.C., Chen, C.H., Lin, C.S., Yang, P.C., Tsay, H.S., and Chen, J.J. (2008). Anticancer effects of tanshinone I in human non-small cell lung cancer. Molecular cancer therapeutics *7*, 3527-3538.
14. Chiu, T.L., and Su, C.C. (2010). Tanshinone IIA induces apoptosis in human lung cancer A549 cells through the induction of reactive oxygen species and decreasing the mitochondrial membrane potential. International journal of molecular medicine *25*, 231-236.
15. Zhang, L., Li, J., Ma, F., Yao, S., Li, N., Wang, J., Wang, Y., Wang, X., and Yao, Q. (2012). Synthesis and cytotoxicity evaluation of 13-n-alkyl berberine and palmatine analogues as anticancer agents. Molecules (Basel, Switzerland) *17*, 11294-11302.
16. Sun, L., Wang, Y et al. (2019). Modelling liver cancer initiation with organoids derived from directly

reprogrammed human hepatocytes. Nature Cell Biology *21*, 1015-1026.

17. Broutier, L., Mastrogiovanni, G., Verstegen, M.M., Francies, H.E., Gavarro, L.M., Bradshaw, C.R., Allen, G.E., Arnes-Benito, R., Sidorova, O., Gaspersz, M.P., *et al.* (2017). Human primary liver cancer-derived organoid cultures for disease modeling and drug screening. Nature Medicinec*23*, 1424-1435.